2010

A New Development Of Feedback Controller For Left Ventricular Assist Device

Yu Wang
University of Central Florida

A NEW DEVELOPMENT OF FEEDBACK CONTROLLER FOR LEFT VENTRICULAR ASSIST DEVICE

by

YU WANG
M.S. Southern Polytechnic State University, 2007
B.S. Dalian University of Technology, 2004

A thesis submitted in partial fulfillment of the requirements
for the degree of Master of Science
in the School of Electrical Engineering and Computer Science
in the College of Engineering and Computer Science
at the University of Central Florida
Orlando, Florida

Summer Term
2010

Major Professor: Marwan A. Simaan

ABSTRACT

The rotary Left Ventricular Assist Device (LVAD) is a mechanical pump surgically implanted in patients with end-stage congestive heart failure to help maintain the flow of blood from the sick heart. The rotary type pumps are controlled by varying the impeller speed to control the amount of blood flowing through the LVAD. One important challenge in using these devices is to prevent the occurrence of excessive pumping of blood from the left ventricle (known as suction) that may cause it to collapse due to the high pump speed. The development of a proper feedback controller for the pump speed is therefore crucial to meet this challenge.

In this thesis, some theoretical and practical issues related to the development of such a controller are discussed. First, a basic nonlinear, time-varying cardiovascular-LVAD circuit model that will be used to develop the controller is reviewed. Using this model, a suction index is tested to detect suction. Finally we propose a feedback controller that uses the pump flow signal to regulate the pump speed based on the suction index and an associated threshold. The objective of this controller is to continuously update the pump speed to adapt to the physiological changes of the patient while at the same time avoiding suction. Simulation results are presented under different conditions of the patient activities. Robustness of the controller to measurement noise is also discussed.

ACKNOWLEDGMENTS

I would like to thank Dr. Marwan A. Simaan, my advisor, for his constant support and many patient suggestions on my study and research. I am also thankful to Dr. Eduardo Divo for his guidance through my early periods of confusion on the work.

I should also give thanks to all other professors and my research teammate, George Faragallah, who gave me much great help for my research.

I specially thank to my parents, for their patience and love, and my wife Cui Jin, who is by my side to give me spiritual support and encouragement all the time.

This work was supported in part by NSF under grant ECCS-0701365. I would like to express my gratitude to them for their financial support.

TABLE OF CONTENTS

LIST OF FIGURES

LIST OF TABLES

CHAPTER 1:INTRODUCTION

According to a survey from World Health Organization, recently cardiovascular diseases occupy around one third of all kinds of diseases. What's worse, this proportion could be much higher in the future and many of these cardiovascular diseases could finally affect the left ventricle [1], which leads to congestive heart failure, a major cardiovascular disease. This disease is a serious case in which the heart cannot pump enough blood to support the body's other organs for patients. Although drug treatments have positive effects to ensure patients' normal lives, a high mortality is still inevitable since this pharmacological therapy often fails in long-term use in real-time; hence, heart transplantation has been an acceptable method to treat serious cases of congestive heart failure.

Patients with congestive heart failure, who are waiting for a heart transplant, often need to wait a long time (around 1 year or more) until a suitable heart becomes available. Furthermore, during this waiting period, patients' already-sick hearts may get worse and become unable to pump enough blood to sustain their lives. Therefore, Left Ventricular Assist Device (LVAD) as "bridge for transplantation" can help a weak heart and "buy time" for patients [2].

Based on the patterns of the blood flow pumped by LVAD, the LVAD can be divided into two main types: positive displacement (pulsatile) and turbo-dynamic (rotary) LVAD. The first

generation of such devices is the pulsatile LVAD that works in a beat-like style to create natural heart flow; as the latest generation of such devices, the rotary LVAD generates continuous blood flow instead of the pulsatile flow. Furthermore, the LVAD can be either used in the in vitro placement, which is percutaneously connected to the patient's heart and artery through the drainage catheter, or implanted in the patient's body (usually in the peritoneal cavity or extra-peritoneal space) [1]. Nowadays the implanted rotary LVAD has been widely applied in clinical practice due to their smaller size, lighter weight, better durability [3], and higher efficiency than conventional pulsatile LVAD.

The rotary LVAD is a mechanical pump surgically implanted from the left ventricle to the aorta to help maintain the flow of blood from the sick heart, which cannot effectively work on its own [2]. The rotary pumps are controlled by changing the rotor speed to control the blood flow through the pump (pump flow). Moreover, the patient with the implanted LVAD even can be discharged from the hospital by automatically regulating the pump speed controlled based on the patient's physiological need, and then have an acceptable quality of life while waiting for an available donor heart.

Two important phenomena, however, must be taken into account regarding the operation for the pump speed of such rotary LVAD: first, if the rotational pump speed is too low, the blood will return from the aorta to the left ventricle, known as "backflow"; second, a high rotational pump

speed may cause suction, a serious event that occurs when the rotary pump attempts to draw much more blood from the left ventricle than available, which can cause the left ventricle to collapse and damage cardiac tissues. Therefore, both two phenomena need to be avoided in practice, especially suction that is much more dangerous.

To achieve the avoidance of suction, two steps are required. The first step is to detect suction. In recent years, several methods have been proposed to solve the suction detection problem. These approaches are mainly based on the specific analysis of certain variables such as pump speed, pump flow, and pump current, which may change drastically when suction occurs. Vollkron and Schima et al. [4, 5] presented several suction indices to detect suction. These suction indicators were based on the time-domain analysis of the pump flow patterns extracted from LVAD-implanted patients under varying physiological conditions. The extracted patterns were compared against previously captured pump flow and classified based on the clinical experience of three human experts in a data base, to determine whether suction is present. This approach, however, also had some intrinsic limitations [4].

Voigt et al. [6] presented a suction detection system with both motor speed and pump current as the continuously accessible signals. The goal of [6] was to evaluate and validate system parameters for this suction detector. When developing the suction detection algorithm, both in

vitro data consisting of pulsatile and non-pulsatile conditions and in vivo data had been considered. The results showed that this method was feasible in the clinical study.

Ferreira et al. [7] described a new suction detection system. In this system, the suction indices were based on the time-domain, frequency-domain, and time-frequency domain and combined to make a decision about the pump flow patterns, which can be correctly classified with the discriminant analysis (DA) approach. This system had been tested with both experimental data and simulation model, indicating good results.

Mason et al. [8] proposed a reliable suction detector with seven time-domain indices from the observed positive spikes induced in the rotational pump speed waveform instead of the pump flow signal, and several different suction index thresholds were set for different patients. The corresponding test had been implemented with both single suction index and paired suction indices, showing that the paired suction indices performed better than the single index.

After detecting suction, the second step is to develop a proper feedback controller such that it can not only automatically adjust the rotational pump to make the pump speed always below the speed when suction occurs, but also provide sufficient cardiac output and perfusion pressure to meet the patient's physiological requirements. Yi Wu et al. [9] presented an advanced physiological controller to prevent suction. This was an optimal proportional integral (PI) based

controller, used to minimize the energy of a nonlinear weighted function of the control input (pump speed) and error signals (difference between referenced and actual output signals). With the nonlinear weighted function, suction can be prevented by this developed PI controller, but this controller adopted a reference aortic pressure as the assumption, which cannot be continuously available in practice.

Vollkron et al [10] discussed the development of a reliable automatic speed control system for implantable rotary blood pumps. A PC-based system that can analyze the pump performance based on the available pump data (i.e., flow, speed, current, and power consumption) was developed. Experimental results indicated that this automatic speed control system can work pretty well even for patients with massive arrhythmia and very thin septal walls.

Shaohui Chen et al. [11, 12] proposed a baroreflex-based feedback controller, which was coupled to a cardiovascular system model. Simulation results showed that this feedback controller can adjust the pump speed based on the Systemic Vascular Resistance (SVR) value considered as the activity level of the patient and Heart Rate (HR) that were under the control of the baroreflex and indicated that this proposed controller can be able to support patients with congestive heart failure under varying physiological conditions. However, there was no suction detection system in this model as the author acknowledged.

Ferreira et al. [13, 14] proposed a control system based on a Fuzzy Logic Controller (FLC). In this system, the suction detector was based on [7] and generated two discriminant scores as the outputs of the suction detector, which were also used as the inputs of FLC. The performance of this control system was tested in the simulations with different Systemic Vascular Resistance (SVR) values, showing that this control system can automatically regulate the pump speed to avoid suction and demonstrating its feasibility. However, the author mentioned that the inclusion of a baroreflex in the system would better represent the behavior of such a controller.

Simaan et al. [15] developed a feedback controller based on the pump flow signal, which was considered as the only continuously measurable variable using current sensor technology. The pump speed was updated based on the slope of the envelope of the minimum pump flow signal within every cardiac cycle. With the onset of suction, the slope of the minimum pump flow envelope was very close to zero. Therefore, this approach was viewed as an extremum seeking algorithm (ESA). The results showed that the proposed controller performed extremely well until very low signal to noise ratios (lower than 20 dB) was added to the pump flow signal.

This thesis reviews and further analyzes the criterion for suction detection in [4], which is called "Mean-Min-Max" that corresponds to the mean, minimum, and maximum values of the pump flow signal that can only be continuously measured with current sensor technology in real-time. This criterion is used to test a suction index, which is then applied to detect suction. A threshold,

related to the suction index, is presented and used with the aforesaid suction index to continuously update the pump speed to meet the patient's need while at the same time preventing suction.

This thesis is organized as follows. Chapter 2 reviews some basic concepts for cardiovascular physiology, a basic cardiovascular circuit model, and a combined cardiovascular-LVAD model then analyzes some simulation results with the cardiovascular-LVAD model. In Chapter 3, the "Mean-Min-Max" criterion is reviewed and its further analysis is described to test a related suction index as the suction detector with both experimental data and simulation model. Chapter 4 discusses the proposed feedback controller and shows related simulation results. Concluding remarks and future work are discussed in Chapter 5.

CHAPTER 2:CARDIOVASCULAR SYSTEM AND MODEL

In this chapter, some basic concepts regarding the heart and cardiovascular physiology that are important to further understand a cardiovascular model with the rotary pump are reviewed. This chapter is organized as follows. Heart and circulatory system are introduced in Section 2.1. Section 2.2 describes the cardiac cycle in details. Section 2.3 reviews a cardiovascular circuit model. In Section 2.4, a combined cardiovascular-LVAD model is reviewed and its open-loop response is simulated by using two different pump speed patterns (step and ramp) and different Systemic Vascular Resistance (SVR) values.

2.1 Heart and Circulatory System

2.1.1 Heart

The heart is an important organ in the circulatory system; it is in the thoracic cavity between left and right lungs. While contracting its size is close to that of the personal fist. The breastbone and costal cartilage are adjacent to the anterior-superior surface of the heart; behind the heart there is the esophagus and the thoracic aorta; the underside of the heart is close to the diaphragm muscle; the upside is the superior vena cava, aorta, and pulmonary artery. Three sulci are on the surface of the heart. The coronary sulcus is the surface demarcation between atria and ventricles; the

anterior-posterior longitudinal sulci are surface demarcations between left and right ventricles. Figure 2.1 shows the anterior and posterior aspects of the heart.

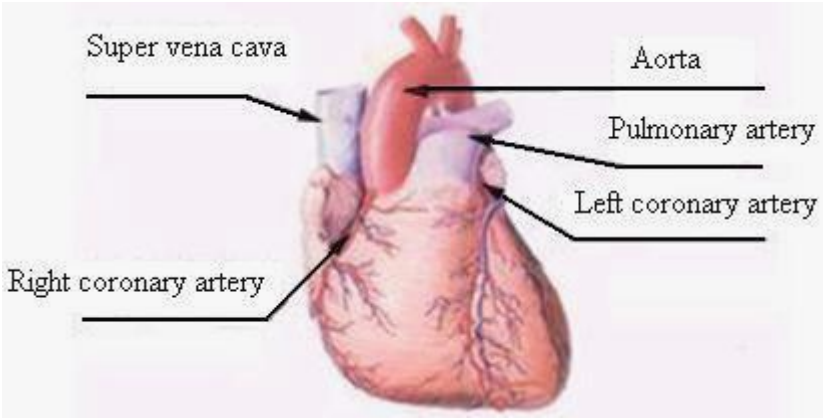

(a)

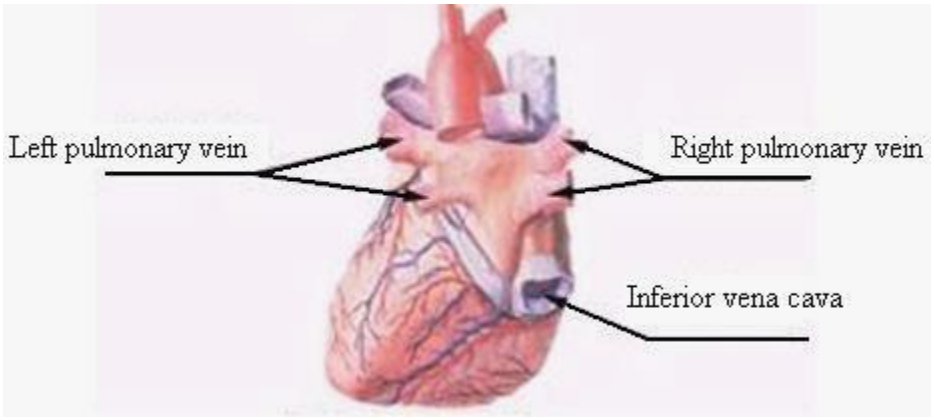

(b)

FIGURE 2.1 Anterior and Posterior Aspects of the Heart [16]

The heart is a hollow organ, which is divided into four chambers: the upper two chambers are atria separated by the atrial septum as left and right atria, respectively; the lower two chambers are ventricles separated by the inter-ventricular septum as left and right ventricles, respectively. Figure 2.2 illustrates the basic structure of the heart.

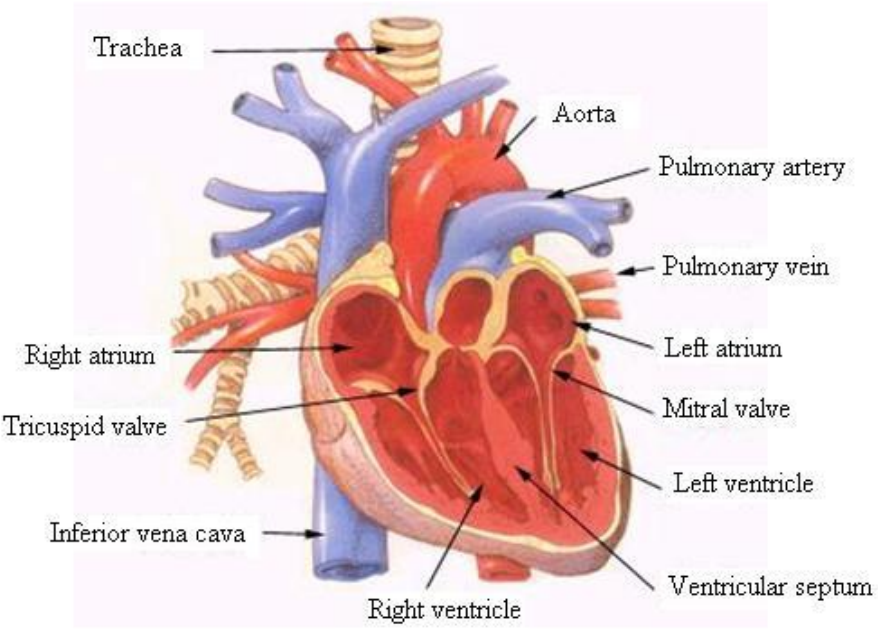

FIGURE 2.2 Basic Structure of the Heart [16]

2.1.2 Circulatory System

The circulatory system consists of the heart and the blood vessels (arteries, arterioles, and blood), whose function is to provide the oxygen and nutrient products to tissues in the body and carry away the byproducts of metabolism. Figure 2.3 describes the block diagram of the circulation process in human's body that is made up of two circulations: systemic and pulmonary circulation.

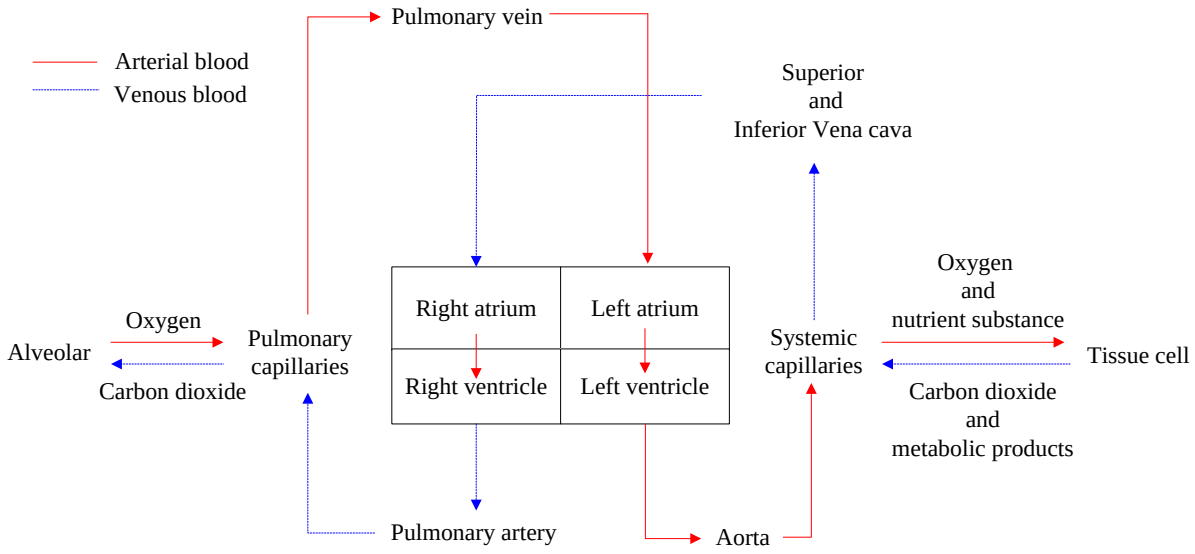

FIGURE 2.3 Block Diagram of Human Circulation Process

Systemic circulation, also known as the major cycle, starts at the left ventricle. When the left ventricle contracts, the arterial blood, including oxygen and nutrient substance, is pumped into the aorta then enters the capillaries via various artery branches. The arterial blood changes into the venous blood that contains carbon dioxide and metabolic products by means of gas and substance exchange in the capillaries with tissues and cells. The venous blood enters the venules through the capillaries and flows into the superior-inferior vena cava and coronary sinus via different-level venous return then goes into the right atrium. After the venous blood flows into the right ventricle from the right atrium, pulmonary circulation begins.

Pulmonary circulation, known as the minor cycle, starts at the right ventricle. With the contraction of the right ventricle, the venous blood is pumped into the pulmonary artery and

reaches into the capillaries in the alveolar wall with all branches of pulmonary arteries, and then the venous blood becomes the arterial blood with oxygen saturation by gas exchange between the blood vessels and alveolar. After that the arterial blood enters the venules through the capillaries and flows into left and right pulmonary veins through venous return at various levels then goes into the left atrium. Finally the arterial blood enters the left ventricle from the left atrium, another systemic circulation will start.

2.2 Cardiac Cycle

2.2.1 Review of Some Basic Concepts

In this section, before discussing the cardiac cycle, some important concepts related to the cardiac cycle are introduced.

Heart Rate (HR): heart rate is the number of heartbeats per unit of time, typically expressed as beats per minute (bpm) that varies depending on the human's age, gender, or body's other physiological need.

Systole: systole is a phase of the cardiac cycle when the heart is contracting, during which the pressure is generated within the atria and ventricles of the heart pumping blood flow. Figure 2.4 shows the ventricular systole.

Diastole: diastole is a phase of the cardiac cycle when the heart is filled with blood after systole.

Figure 2.5 shows the ventricular diastole.

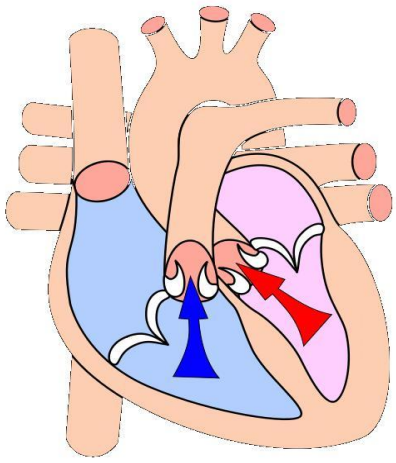

FIGURE 2.4 Ventricular Systole [17]

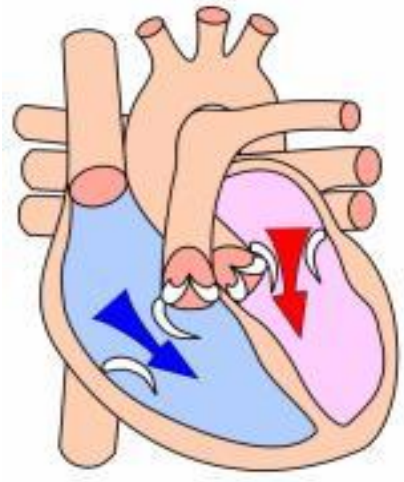

FIGURE 2.5 Ventricular Diastole [18]

Stroke Volume (SV): stroke volume is the volume of blood pumped from one ventricle of the heart with each beat. It is equally available for both the left and right ventricles of the heart. The expression is as follows:

$$SV = EDV - ESV \tag{2.1}$$

Where EDV is the end-diastolic volume, the volume of blood in the ventricle prior to a beat, and ESV is the end-systolic volume, the volume of blood at the end of a beat.

Cardiac Output (CO): cardiac output is the volume of blood pumped by the ventricle in a minute, it is the product of stroke volume and heart rate such that

$$CO = SV * HR \tag{2.2}$$

Preload: preload, also known as the volume load, is thought of as the “load” before the cardiac muscle starts contracting.

Afterload: afterload, also known as the pressure load, is defined as the "resistance" that the heart begins to contract and eject blood against.

2.2.2 Heart Cycle

The cardiac cycle is a period of time between two consecutive heart beats. For example, for a normal heart, if the heart rate is 75bpm, the heart cycle is 0.8 s. One cardiac cycle contains two main phases: systole (contraction) and diastole (relaxation) for both atrium and ventricle. However, during the cardiac pumping, the ventricle can play a major role compared with the atrium. Therefore, the cardiac cycle often means the activity cycle for the ventricle.

Figure 2.6 illustrates the changes of several important hemodynamic variables: Left Ventricular Pressure (LVP), Aortic Pressure (AoP), Left Atrial Pressure (LAP), and Left Ventricular Volume (LVV) during one cardiac cycle and takes into account the left ventricle as an example. In order to discuss a complete cardiac cycle in details, one cardiac cycle can be divided into 8 phases [19] (see Figure 2.6):

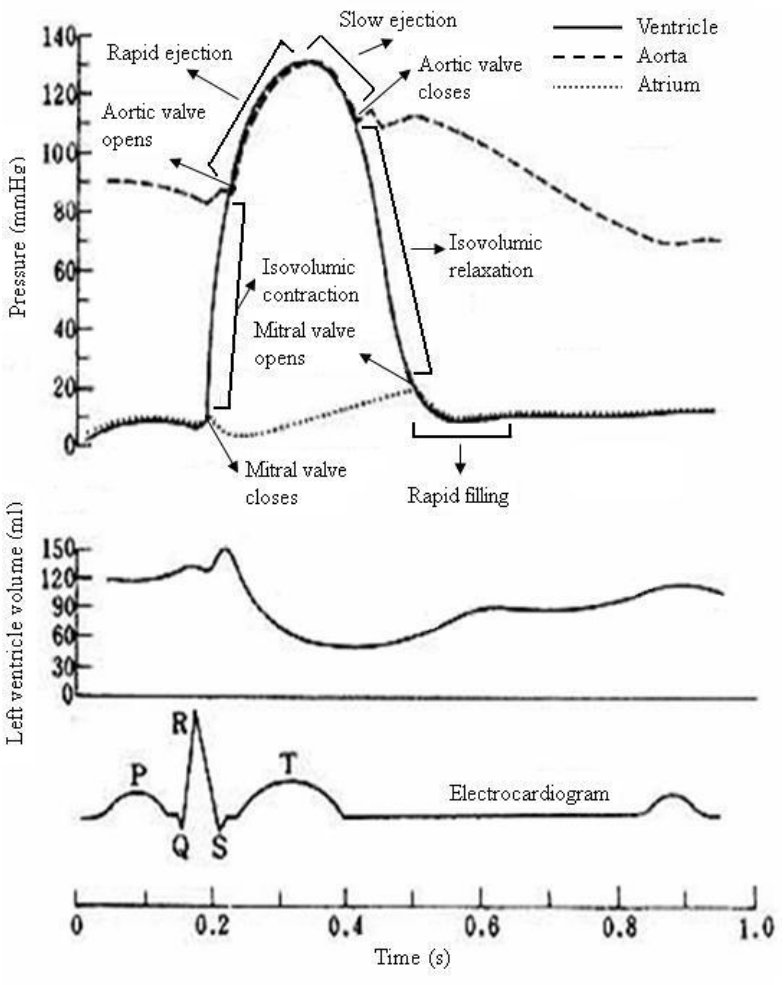

FIGURE 2.6 LVP, AoP, AP, and LVV in One Cardiac Cycle [19]

Phase 1: isovolumic contraction. The left ventricle starts contracting when R wave of QRS complex that represents the potential and time changes in the ventricular depolarization and most primitive repolarization in the electrocardiogram (see Figure 2.6) reaches its peak value. The left ventricular pressure sharply increases due to the powerful contraction of the ventricular myocardium. When the left ventricular pressure overcomes the left atrial pressure, the blood in the left ventricle impels the corresponding mitral valve in the left atrio-ventricular orifice to

make it closed. The mitral valve is tightened by the papillary muscle and chordae tendineae, and the contraction of the ring muscle decreases the caliber in the atrio-ventricular junction area, hence the blood in the left atrium is prevented from regurgitating into the left atrium. At this point, the left ventricular pressure increases fast but when it doesn't exceed the aortic pressure (around 80 mmHg in end-systole), the aortic valve in the aorta orifice is still closed. During this short period (normally 0.05 s), both mitral and aortic valves are not open, the size between the apex and base of the heart decreases, the left ventricle turns round, the tension of the ventricular myocardium enhances but the left ventricular volume is not changed, this is called isovolumic contraction.

Phase 2: rapid ejection. The ventricular myocardium keeps contracting and its tension continues to enhance, causing the left ventricular pressure to exceed the aortic pressure shortly then the aortic valve is blown out, the blood is ejected into the aorta and reaches its maximum flow velocity fast. During end-rapid ejection the left ventricular pressure can reach its peak value (120-130 mmHg in the left ventricle). In this phase it takes only 0.09 s but the volume of ejected blood occupies 80%-85% of stroke volume.

Phase 3: slow ejection. During this period, the contractility of the left ventricle is weak, the left ventricular pressure decreases, the ejection velocity becomes slow. Although the left ventricular pressure is a little less than the aortic pressure (only several mmHg), the total energy in the left

ventricle (pressure energy plus kinetic energy) is still larger than that in the aorta due to the ventricular contraction. Therefore, the blood can continue to be ejected from the left ventricle. This phase uses 0.13 s on average then the cardiac cycle goes into the phase of diastole (relaxation).

Phase 4: pre-diastole. The left ventricle begins to relax and the ejection stops, the left ventricular pressure suddenly drops. As discussed in phase 3, the left ventricular pressure is smaller than the aortic pressure and the aortic valve is quickly shut down to stop the blood regurgitating into the left ventricle, hence the period from the onset of the ventricular diastole to the closure of the aortic valve is called pre-diastole with the duration of 0.04 s.

Phase 5: isovolumic relaxation. When the aortic valve is closed the left ventricular pressure still overcomes the left atrial pressure, so the mitral valve remains closed, which will not be open until the left ventricular pressure keeps dropping to be below the left atrial pressure. During this short phase (0.08 s), the left ventricular pressure sharply decreases but the left ventricular volume is basically constant, which is the phase of isovolumic relaxation.

Phase 6: rapid filling. With the mitral valve opening, the left ventricular volume increases fast and the left ventricular pressure is much lower than the left atrial pressure, making the blood in the left atrium and great cardiac veins rapidly flow into the left ventricle with a period of 0.11 s, during this period two-thirds of blood in the left ventricle is filling.

Phase 7: slow filling (end diastole). With the blood in the left ventricle rapidly filling, the velocity of blood flow in veins entering back to the left ventricle via the left atrium gradually decreases, the pressure difference between the left atrium and the left ventricle decreases but the left ventricular volume is still increasing, this phase is called slow filling that takes about 0.19 s then the left atrium starts contracting.

Phase 8: atrium contraction. The left atrium contracts by the end of the ventricle diastole, the remaining blood in the left atrium is ejected into the left ventricle because of the increasing left atrial pressure, improving the fullness degree of the left ventricle and increasing the left ventricular pressure. When the left atrium contracts, it makes the left atrial pressure decrease, helping close the mitral valve, so before the left ventricle contracts, the mitral valve has the tendency to be closed. Therefore, before next isovolumic contraction, the aforementioned 8 phases form a complete cardiac cycle.

2.3 Cardiovascular Model

The heart is known as a time-varying and nonlinear system. In order to simulate the heart, numerous simplified and complex mathematical models of the cardiovascular system have been studied for several years. Yi Wu et al. [9] modeled a complicated bi-ventricular human cardiovascular system. Shaohui Chen [11] used a simplified uni-ventricular model of the cardiovascular system in state space form that was developed by using a minimal number of state

variables to make the system identification as simple as possible; Simaan et al. [15] proposed a modified cardiovascular model, consisting of five state variables with the assumption that both pulmonary circulation and the right ventricle can work normally, hence their effect can be neglected. In this research, Simaan's model is adopted. The specific model, state equations, and relative simulation results are discussed in this section.

2.3.1 Cardiovascular Circuit Model

A cardiovascular equivalent circuit model is shown in Figure 2.7. In this model, Preload and pulmonary circulations are represented by a single capacitor C_R, and afterload is described as a four-element windkessel model that consists of R_S, R_C, C_S, and L_S. Notice that in [11] there was no capatitor C_A, representing the aortic compliance used in this model. The mitral valve is described as a resistor R_M and an ideal diode D_M, and the aortic valve is represented by a resistor R_A and an ideal diode D_A. Table 2.1 lists the state variables and Table 2.2 lists all the system parameters in Figure 2.7 and their corresponding values [11-15].

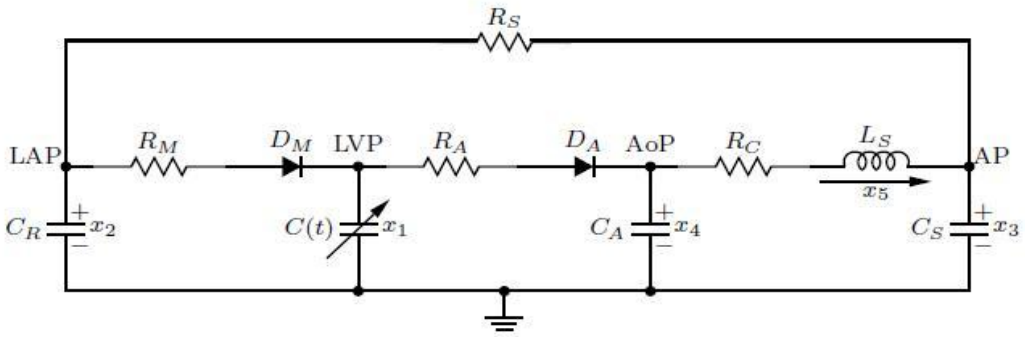

FIGURE 2.7 Cardiovascular Circuit Model

TABLE 2.1 State Variables of Cardiovascular Model

Variables	Name	Physiological Meaning (units)
$x_1(t)$	LVP(t)	Left Ventricular Pressure (mmHg)
$x_2(t)$	LAP(t)	Left Atrial Pressure (mmHg)
$x_3(t)$	AP(t)	Arterial Pressure (mmHg)
$x_4(t)$	AoP(t)	Aortic Pressure (mmHg)
$x_5(t)$	QT(t)	Total Flow (ml/s)

TABLE 2.2 Model Parameters for Cardiovascular Model

Parameters	Value	Physiological Meaning
R_S (mmHg.s/ml)	1.0	Systemic Vascular Resistance (SVR)
R_M (mmHg.s/ml)	0.005	Mitral Value Resistance
R_A (mmHg.s/ml)	0.001	Aortic Value Resistance
R_C (mmHg.s/ml)	0.0398	Characteristic Resistance
C(t) (ml/mmHg)	Time-varying	Left Ventricular Compliance
C_R (ml/mmHg)	4.4	Left Atrial Compliance
C_S (ml/mmHg)	1.33	Systemic Compliance
C_A (ml/mmHg)	0.08	Aortic Compliance
L_S (mmHg.s^2/ml)	0.0005	Inertance of Blood in Aorta
D_M		Mitral Value
D_A		Aortic Value

In this model, the left ventricle is represented by a time-varying compliance C(t). In order to model its response, one way is to use the ventricle's elastance function E(t), which is the reciprocal of C(t) and associated with the contractility of the heart. The elastance theory was presented by Suga and Sagawa [20]. It is defined as the ratio of the left ventricular pressure (LVP) to the left ventricular volume (LVV), which means to describe the relationship between pressure and volume of the left ventricle such that

$$E(t) = \frac{LVP(t)}{LVV(t) - V_0} = \frac{1}{C(t)} \tag{2.3}$$

Where V_0 is a reference volume, the theoretical volume in the ventricle at zero pressure (10 ml for a normal heart).

Some mathematical derivations have been used to describe the elastance function E(t). In this model, a so called "double hill" function [21] is used, whose expression is as follows:

$$E_n(t_n) = 1.55 * \left[\frac{\left(\frac{t_n}{0.7}\right)^{1.9}}{1 + \left(\frac{t_n}{0.7}\right)^{1.9}} \right] * \left[\frac{1}{1 + \left(\frac{t_n}{1.17}\right)^{21.9}} \right] \tag{2.4}$$

The scaled elastance function is defined as

$$E(t) = (E_{\max} - E_{\min}) E_n(t_n) + E_{\min} \tag{2.5}$$

In equation (2.5), constants E_{max} and E_{min} are related to the end-systolic pressure volume relationship (ESPVR) and the end-diastolic pressure volume relationship (EDPVR), respectively, E(t) is a re-scaled version of $E_n(t_n)$, the normalized elastance. In addition, $t_n = t/T_{max}$, $T_{max} = 0.2 + 0.15t_c$, and t_c is the cardiac cycle interval (i.e., $t_c = 60/HR$), where HR is the heart rate discussed in Section 2.2. Figure 2.8 shows the elastance function E(t) with E_{max} = 2 mmHg/ml, E_{min} = 0.06 mmHg/ml, and HR = 75 bpm as a normal heart.

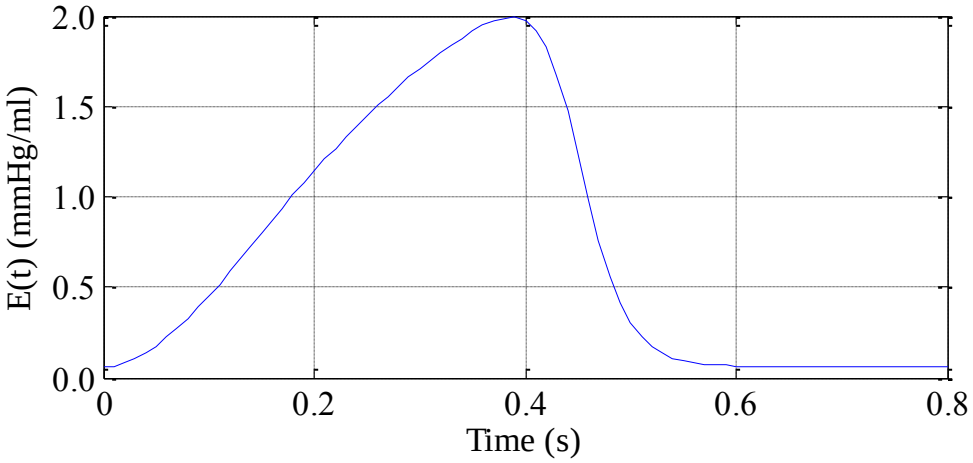

FIGURE 2.8 Elastance Function E(t)

TABLE 2.3 Phases of Cardiac Cycle

Modes	Valves		Phases
	D_M	D_A	
1	closed	closed	Isovolumic contraction
2	closed	open	Ejection
1	closed	closed	Isovolumic relaxation
3	open	closed	Filling
-	open	open	Not feasible

From the analysis of the cardiac cycle in Section 2.2.2, the mitral and aortic valves can determine the phases of the cardiac cycle. In view of this work, the phases can be divided into three different modes (isovolumic contraction and relaxation, ejection, filling) with the open and closed states of the mitral and aortic valves. Notice that it is not feasible to open both mitral and aortic valves. Table 2.3 lists the phases of the cardiac cycle.

2.3.2 State Equations

According to Table 2.3, since there are three available modes, three sets of differential equations for describing this cardiovascular model for every mode can be derived. However, as the nonlinear elements of the two diodes, one feasible way to describe this model is to write only one set of state equations by using some basic circuit analysis methods such as KVL and KCL, hence the state equations for this time-varying and nonlinear cardiovascular circuit model shown in Figure 2.7 can be derived as followed:

$$\dot{x} = f(x,t) = A_c(t)x + P_c(t)P(x) \tag{2.6}$$

Where $A_c(t)$ and $P_c(t)$ are (5×5) and (5×2) time-varying matrices, respectively, and P(x) is a (2×1) vector, used to model the nonlinear behavior of the two diodes previously mentioned. Note that the expression of $P_c(t)$ is not associated with the three modes such that

$$P_c(t) = \begin{bmatrix} \frac{1}{C(t)} & \frac{-1}{C(t)} \\ \frac{-1}{C_R} & 0 \\ 0 & 0 \\ 0 & \frac{1}{C_A} \\ 0 & 0 \end{bmatrix} \tag{2.7}$$

Both $A_c(t)$ and P(x) are changed with respect to the three different modes previously discussed.

Mode 1: Isovolumic phase.

$$A_c(t) = \begin{bmatrix} \frac{-\dot{C}(t)}{C(t)} & 0 & 0 & 0 & 0 \\ 0 & \frac{-1}{R_s C_R} & \frac{1}{R_S C_R} & 0 & 0 \\ 0 & \frac{1}{R_S C_S} & \frac{-1}{R_S C_S} & \frac{1}{C_S} & 0 \\ 0 & 0 & 0 & 0 & \frac{-1}{C_A} \\ 0 & 0 & \frac{-1}{L_S} & \frac{1}{L_S} & \frac{-R_C}{L_S} \end{bmatrix} \tag{2.8}$$

$$P(x) = \begin{bmatrix} 0 \\ 0 \end{bmatrix} \tag{2.9}$$

Mode 2: Ejection phase.

$$A_c(t)=\begin{bmatrix} \frac{-\dot{C}(t)}{C(t)}-\frac{1}{C(t)R_A} & 0 & 0 & \frac{1}{C(t)R_A} & 0 \\ 0 & \frac{-1}{R_sC_R} & \frac{1}{R_SC_R} & 0 & 0 \\ 0 & \frac{1}{R_SC_S} & \frac{-1}{R_SC_S} & 0 & \frac{1}{C_S} \\ \frac{1}{C_AR_A} & 0 & 0 & \frac{-1}{C_AR_A} & \frac{-1}{C_A} \\ 0 & 0 & \frac{-1}{L_S} & \frac{1}{L_S} & \frac{-R_C}{L_S} \end{bmatrix} \tag{2.10}$$

$$P(x)=\begin{bmatrix} 0 \\ \frac{r(x_1-x_4)}{R_A} \end{bmatrix} \tag{2.11}$$

Mode 3: Filling phase.

$$A_c(t)=\begin{bmatrix} \frac{-\dot{C}(t)}{C(t)}-\frac{1}{C(t)R_M} & \frac{1}{C(t)R_M} & 0 & 0 & 0 \\ \frac{1}{R_MC_R} & \frac{-1}{C_R}(\frac{1}{R_M}+\frac{1}{R_S}) & \frac{1}{R_SC_R} & 0 & 0 \\ 0 & \frac{1}{R_SC_S} & \frac{-1}{R_SC_S} & 0 & \frac{1}{C_S} \\ 0 & 0 & 0 & 0 & \frac{-1}{C_A} \\ 0 & 0 & \frac{-1}{L_S} & \frac{1}{L_S} & \frac{-R_C}{L_S} \end{bmatrix} \tag{2.12}$$

$$P(x)=\begin{bmatrix} \frac{r(x_2-x_1)}{R_M} \\ 0 \end{bmatrix} \tag{2.13}$$

Where r(x) is the ramp function:

$$r(x)=\begin{cases} x, & if \quad x \geq 0 \\ 0, & if \quad x < 0 \end{cases} \tag{2.14}$$

2.3.3 Simulation Results

In order to check the performance of the above cardiovascular circuit model, simulation tests have been implemented by MATLAB. Figure 2.9 illustrates the simulation results of several hemodynamic variables in the model such as LVP, LAP, AoP, QT, and LVV (cardiac cycle is 0.8 s). Ferreira [13] completed the model validation with three different methods.

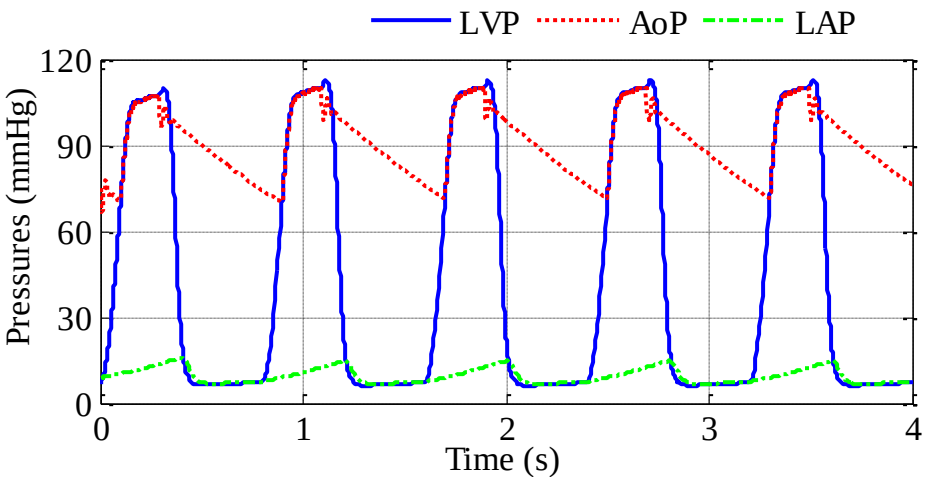

(a)

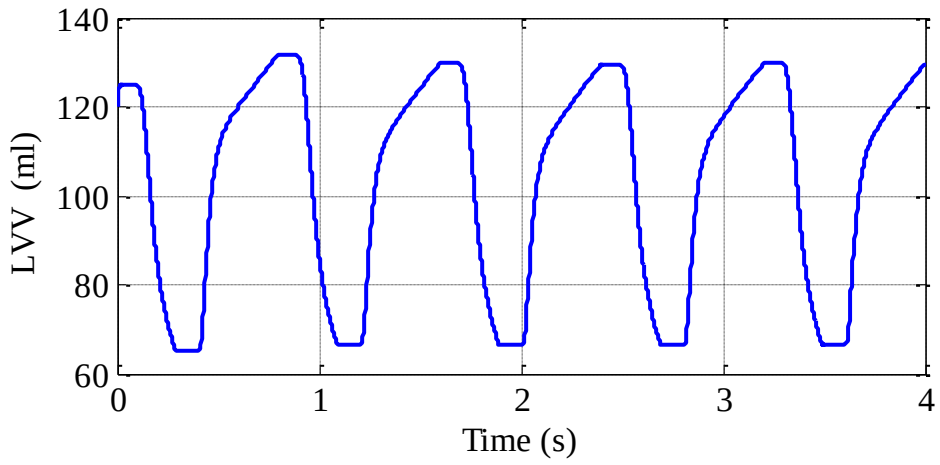

(b)

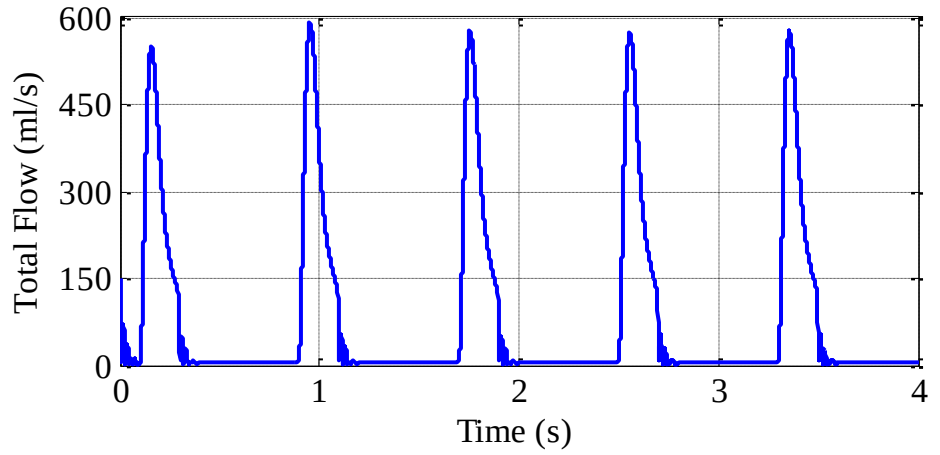

(c)

FIGURE 2.9 Simulation of Main Hemodynamic Parameters for a Normal Heart

2.4 The Combined Cardiovascular-Pump Model

When patients are with end-stage congestive heart failure, heart transplantation is the best therapy. Many of the patients, however, may die during their waiting period before getting an available donor heart. Therefore, the medical community has laid great emphasis on the use of

mechanical assist devices that can substitute for the sick heart. The LVAD is such a device. Figure 2.10 shows a schematic of a rotary LVAD. In this section, a cardiovascular-LVAD model in [15] is reviewed with the corresponding state equations. After that the open-loop response is simulated and analyzed under different conditions of various pump speed patterns and varying Systemic Vascular Resistance (SVR) values.

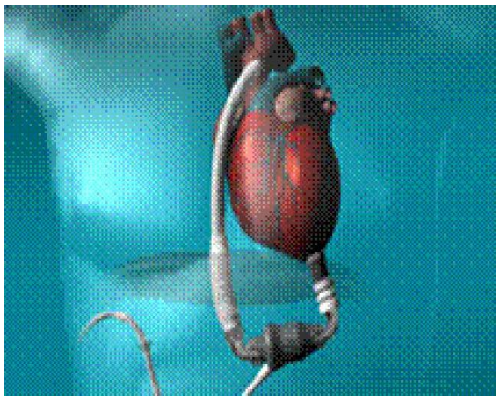

FIGURE 2.10 Schematic of a Rotary LVAD [15]

2.4.1 Cardiovascular-LVAD Model

A combined cardiovascular-LVAD model is shown in Figure 2.11. Compared with the model in Figure 2.7, this combined model connects a rotary pump from the left ventricle to the aorta, consisting of the new state variable (x_6) that represents the blood flow through the pump (i.e., pump flow) and five passive parameters (x_1 through x_5) previously presented in Section 2.3. Table 2.4 lists the state variables of this cardiovascular-LVAD model. Table 2.5 lists all the parameters with their related values for the LVAD.

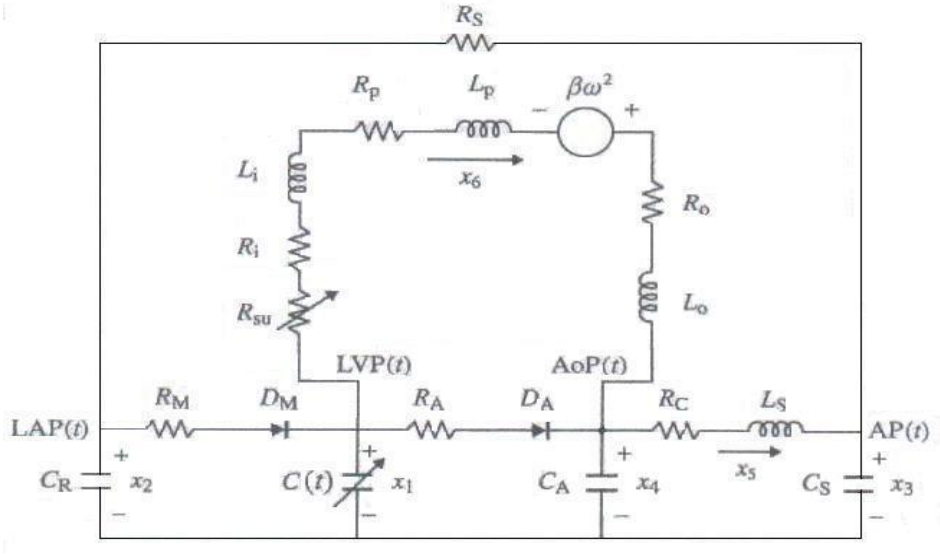

FIGURE 2.11 Cardiovascular-LVAD Circuit Model [22]

TABLE 2.4 State Variables of the Combined Model

Variables	Name	Physiological Meaning (units)
$x_1(t)$	LVP(t)	Left Ventricular Pressure (mmHg)
$x_2(t)$	LAP(t)	Left Atrial Pressure (mmHg)
$x_3(t)$	AP(t)	Arterial Pressure (mmHg)
$x_4(t)$	AoP(t)	Aortic Pressure (mmHg)
$x_5(t)$	QT(t)	Total Flow (ml/s)
$x_6(t)$	PF(t)	Pump Flow (ml/s)

TABLE 2.5 Model Parameters for the LVAD Model

Parameters	Value	Physiological Meaning
R_{SU} (mmHg.s/ml)	See (2.15)	Suction Resistance with parameters:
R_i (mmHg.s/ml)	0.0677	Inlet Resistance of Cannulae
R_O (mmHg.s/ml)	0.0677	Outlet Resistance of Cannulae
L_i (mmHg.s^2/ml)	0.0127	Inlet Inertance of Cannulae
L_O (mmHg.s^2/ml)	0.0127	Outlet Inertance of Cannulae
R_P	0.1707	Pressure Difference Parameter
L_P	0.02177	Pressure Difference Parameter
β	0.00000099025	Pressure Difference Parameter

In Figure 2.11, R_{su} is a special term, called suction element model developed by Schima et al. [23]. It is an empirical model such that its resistance varies with the Left Atrial Pressure (LAP), which is zero when LAP is larger than a given threshold and linearly increases if LAP is below that threshold at a given rate. In another word, this suction model is a pressure-dependent resistance.

Ferreira [13], Simaan [15], and several other researchers used a modified version of Schima's suction model. In this case, the value of the suction resistance is related to the left ventricular

pressure (i.e., $x_1(t)$ in the cardiovascular-LVAD model) instead of the left atrial pressure. This modified suction model is adopted in this combined model. In Figure 2.11 resistor R_{su} is used to express the suction resistance with two parameters, the mathematical expression and the values of the two parameters are given as

$$R_{su} = \begin{cases} 0, & if\ x_1(t) > \overline{x_1} \\ \alpha(x_1(t) - \overline{x_1}) & if\ x_1(t) \le \overline{x_1} \end{cases} \tag{2.15}$$

Where α is -3.5 s/ml and $\overline{x_1}$ is 1 mmHg.

2.4.2 State Equations

According to the state equations in Section 2.3.2, the state equations for this combined cardiovascular-LVAD model can be written as

$$\dot{x} = f(x,t,u) = A_c(t)x + P_c(t)P(x) + bu(t) \tag{2.16}$$

Where $A_c(t)$ and $P_c(t)$ are (6×6) and (6×2) time-varying matrices, respectively. P(x) is the same as that shown in Section 2.3.2 and $P_c(t)$ is expressed as follows:

$$P_c(t) = \begin{bmatrix} \frac{1}{C(t)} & \frac{-1}{C(t)} \\ \frac{-1}{C_R} & 0 \\ 0 & 0 \\ 0 & \frac{1}{C_A} \\ 0 & 0 \\ 0 & 0 \end{bmatrix} \tag{2.17}$$

In addition, $u(t) = \omega^2(t)$, $\omega(t)$ is the rotational speed of the pump as the control variable, and b is a (6×1) vector, given as

$$b = \begin{bmatrix} 0 & 0 & 0 & 0 & 0 & \beta / L^* \end{bmatrix}^T \tag{2.18}$$

$A_c(t)$ varies according to the three different modes mentioned previously.

Mode 1: Isovolumic phase.

$$A_c(t) = \begin{bmatrix} \frac{-\dot{C}(t)}{C(t)} & 0 & 0 & 0 & 0 & \frac{-1}{C(t)} \\ 0 & \frac{-1}{R_S C_R} & \frac{1}{R_S C_R} & 0 & 0 & 0 \\ 0 & \frac{1}{R_S C_S} & \frac{-1}{R_S C_S} & \frac{1}{C_S} & 0 & 0 \\ 0 & 0 & 0 & 0 & \frac{-1}{C_A} & \frac{1}{C_A} \\ 0 & 0 & \frac{-1}{L_S} & \frac{1}{L_S} & \frac{-R_C}{L_S} & 0 \\ \frac{1}{L^*} & 0 & 0 & \frac{-1}{L^*} & 0 & \frac{-R^*}{L^*} \end{bmatrix} \tag{2.19}$$

Mode 2: Ejection phase.

$$A_c(t) = \begin{bmatrix} \frac{-\dot{C}(t)}{C(t)} - \frac{1}{C(t)R_A} & 0 & 0 & \frac{1}{C(t)R_A} & 0 & \frac{-1}{C(t)} \\ 0 & \frac{-1}{R_S C_R} & \frac{1}{R_S C_R} & 0 & 0 & 0 \\ 0 & \frac{1}{R_S C_S} & \frac{-1}{R_S C_S} & \frac{1}{C_S} & 0 & 0 \\ \frac{1}{C_A R_A} & 0 & 0 & \frac{-1}{C_A R_A} & \frac{-1}{C_A} & \frac{1}{C_A} \\ 0 & 0 & \frac{-1}{L_S} & \frac{1}{L_S} & \frac{-R_C}{L_S} & 0 \\ \frac{1}{L^*} & 0 & 0 & \frac{-1}{L^*} & 0 & \frac{-R^*}{L^*} \end{bmatrix} \quad (2.20)$$

Mode 3: Filling phase.

$$A_c(t) = \begin{bmatrix} \frac{-\dot{C}(t)}{C(t)} - \frac{1}{C(t)R_M} & \frac{1}{C(t)R_M} & 0 & 0 & 0 & \frac{-1}{C(t)} \\ \frac{-1}{R_M C_R} & \frac{-1}{C_R}(\frac{1}{R_M} + \frac{1}{R_S}) & \frac{1}{R_S C_R} & 0 & 0 & 0 \\ 0 & \frac{1}{R_S C_S} & \frac{-1}{R_S C_S} & \frac{1}{C_S} & 0 & 0 \\ 0 & 0 & 0 & 0 & \frac{-1}{C_A} & \frac{1}{C_A} \\ 0 & 0 & \frac{-1}{L_S} & \frac{1}{L_S} & \frac{-R_C}{L_S} & 0 \\ \frac{1}{L^*} & 0 & 0 & \frac{-1}{L^*} & 0 & \frac{-R^*}{L^*} \end{bmatrix} \quad (2.21)$$

Where $$L^* = L_i + L_O + L_P \quad (2.22)$$

$$R^* = R_i + R_O + R_{SU} + R_P \quad (2.23)$$

2.4.3 Open Loop Simulations

In the open loop simulations, the value of E_{max} equals to 1.0 mmHg/ml for a sick heart since E_{max} is considered to be 2.0 mmHg/ml for a healthy heart in this cardiovascular-LVAD model. In addition, equation (2.2) will not available any more since the pump can replace the natural heart to provide continuous blood flow. The actual cardiac output will be the combination of the blood flow pumped by the heart and that through the LVAD.

Figure 2.12 illustrates a step response simulation. In this test, the pump speed ω varies from 8000 to 10000 rpm. In Figure 2.12 (b), as the pump speed increases, the amplitude of the pump flow becomes small.

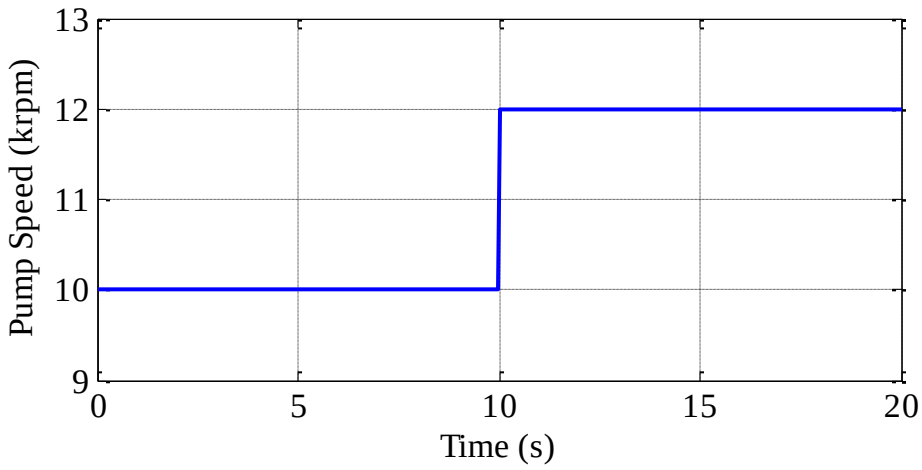

(a)

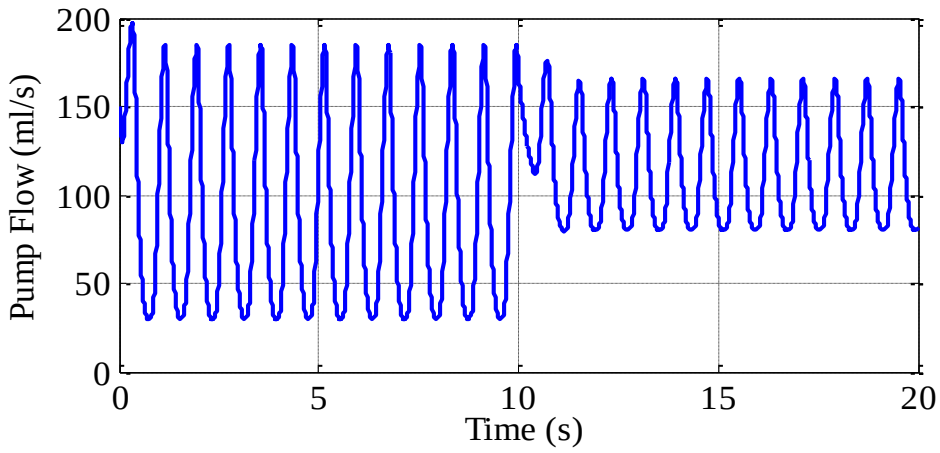

(b)

FIGURE 2.12 Step Response Simulations for the Combined Model

Figure 2.13 shows the effect of the ramp pump speed on LVP, AoP, QT, and PF. The ramp pump speed linearly increases, starting at 12000 rpm with the slope of 100 over the period of 20 seconds. In Figure 2.13 (b), note that AoP is larger than LVP at all time since the aortic valve is not open during the ejection, in fact the phases of the aortic valve (i.e., open or closed) depends on the contractility strength of the heart and the value of the pump speed. In this case since the weak left ventricle is not strong enough to open the aortic valve, the cardiac output (total flow) is equal to the pump flow, meaning that the cardiac output is totally provided by the LVAD. This can also be proven in Figure 2.13 (c).

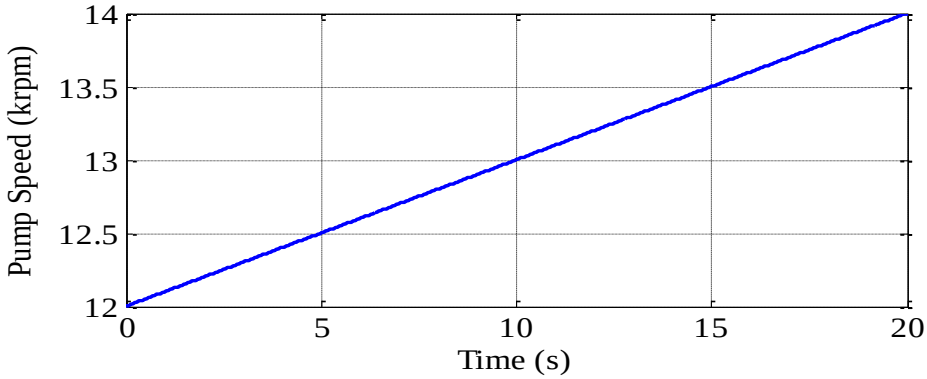

(a)

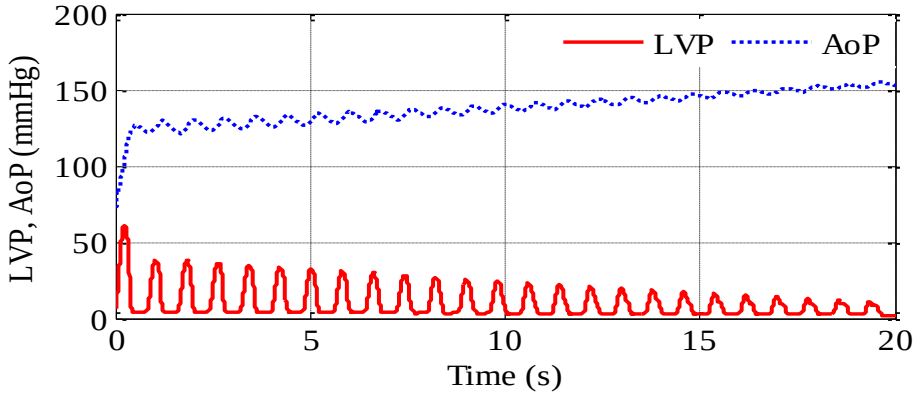

(b)

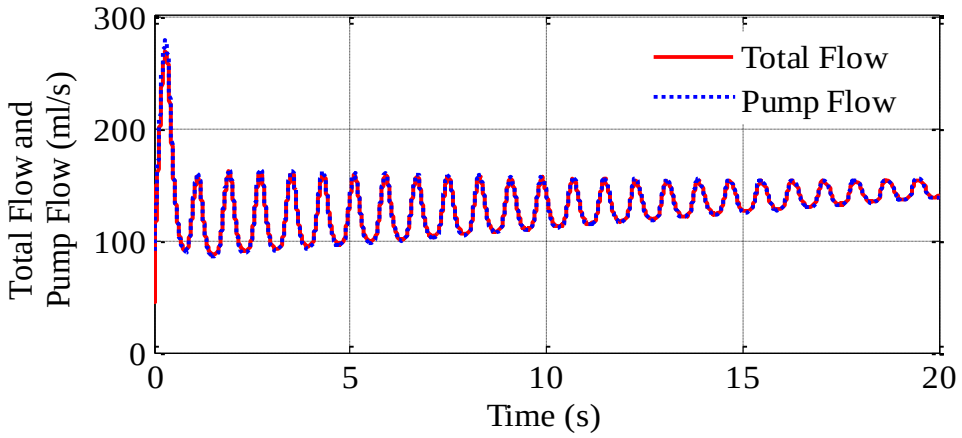

(c)

FIGURE 2.13 Simulations of Ramp Pump Speed, LVP, AoP, QT, and PF

In the cardiovascular-LVAD model, R_S is a critical element, whose physiological meaning is the Systemic Vascular Resistance (SVR), representing the patient activity level. In this work, R_S is set at 1.0 mmHg.s/ml as the baseline level used in both Figures 2.12 and 2.13. When R_S increases, it represents a drop in the patient activity level (i.e., a patient who is running then sitting down for a rest). Correspondingly, the decrease in R_S can be viewed as a rise in the level of activity of the patient. In cardiovascular physiology, it is defined as the resistance, offered by the peripheral circulation to the blood flow. To a great extent, the pump flow is associated with R_S. Figure 2.14 (a) shows the pump flow signal with R_S = 0.5 mmHg.s/ml as the exercise condition and Figure 2.14 (b) shows the pump flow signal with R_S = 1.2 mmHg.s/ml as the rest condition, respectively. The pump speed is the same as shown in Figure 2.13 (a).

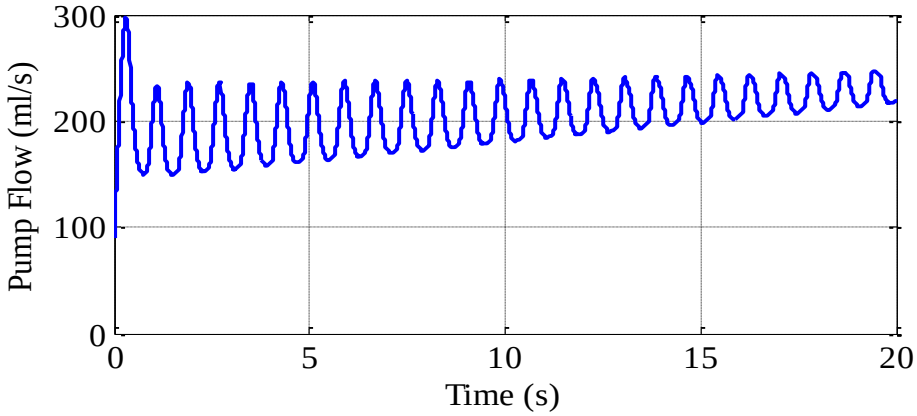

(a) R_S = 0.5 mmHg.s/ml

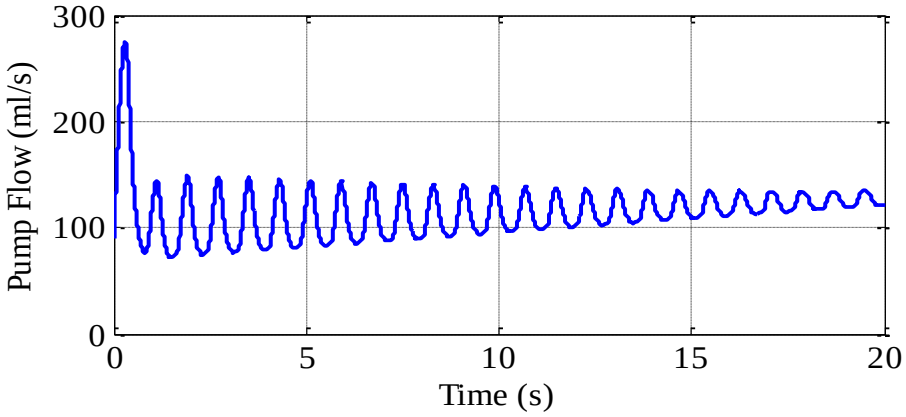

(b) R_S = 1.2 mmHg.s/ml

FIGURE 2.14 Pump Flow Signal with Different R_S

In Figure 2.14, clearly under the higher level of activity of the patient (i.e., at the exercise level with R_S = 0.5 mmHg.s/ml), both maximum and minimum values of the pump flow signals within each cardiac cycle will be larger than these when the level of activity of the patient is lower (R_S = 1.2 mmHg.s/ml). These responses are reasonable since when people are doing some exercises, the activity of the heart is more strenuous than normal; as a result, more cardiac output is needed to meet the body's requirements. If people are having a rest, there is little cardiac output required compared with that under both normal and exercise conditions.

CHAPTER 3:SUCTION DETECTION PROBLEM IN LVAD

The suction phenomenon is known as one of the major complications in the development of implantable rotary blood pumps. Suction can be defined as the collapse of the ventricle or tissues and cells damage. The reason is that the pumped blood outflow exceeds the blood flow to the heart, which means the heart is over-pumping more blood than normally needed. Figure 3.1 shows the normal and collapsed ventricle sacs in a mock loop experiment that simulates a healthy ventricle and an auxiliary pump with a pneumatically actuated artificial heart and an unsealed centrifugal pump, respectively [24].

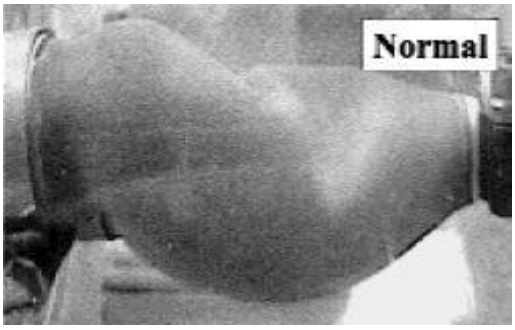

(a)

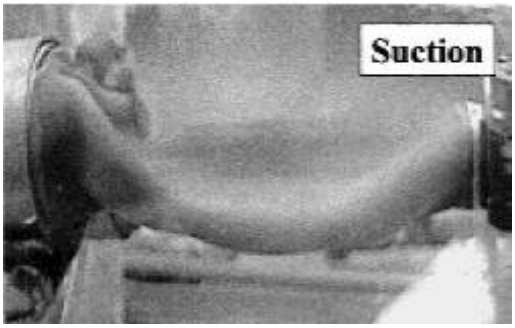

(b)

FIGURE 3.1 Ventricle Sacs [24]

Therefore, the suction detection is a crucial procedure before developing a proper feedback controller for LVAD. To achieve this, a common task is to extract some features from available related signals. This chapter is organized as follows. Section 3.1 describes the suction phenomenon with both experimental data and model simulation. Section 3.2 reviews and extendedly analyzes one of the suction detection approaches in [4, 5] to test a suction index as the suction detector in this thesis. Section 3.3 discusses the simulation results of the suction index coupled to the cardiovascular-pump model shown in Chapter 2.

3.1 Suction Problem in LVAD

Figure 3.2 illustrates an example of the pump speed and pump flow signal of an animal in-vivo test[1] performed using a calf experiment at University of Pittsburgh with the WorldHeart[2] LVAD. The data is sampled at a rate of 500Hz and the heart cycle is 0.9 s.

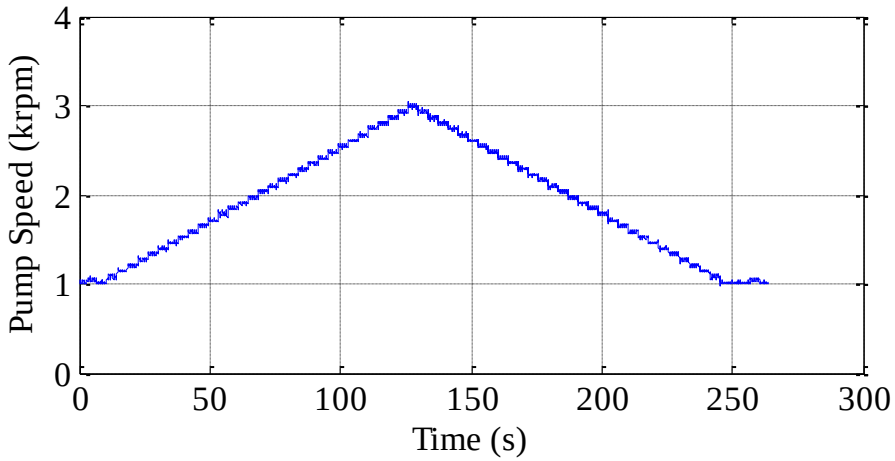

(a)

[1] Authorized according to WorldHeart, Inc. IRB DO 01-06002.
[2] WorldHeart, Inc., formely MedQuest, Inc., Salt Lake City, UT.

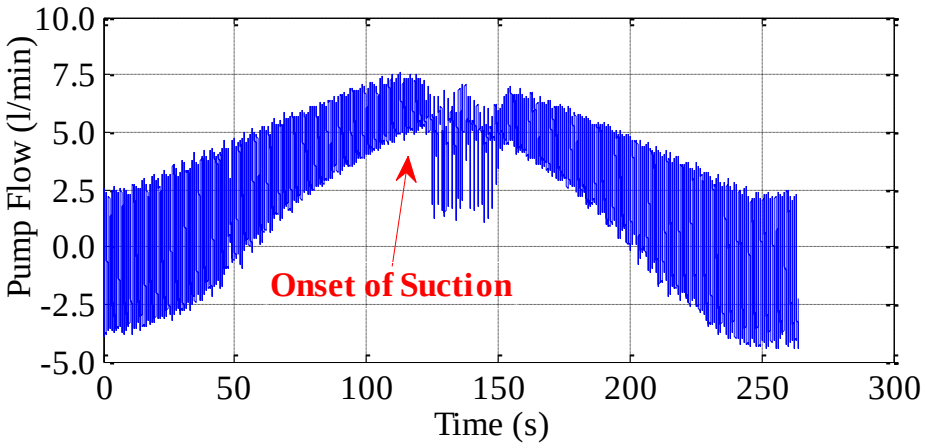

(b)

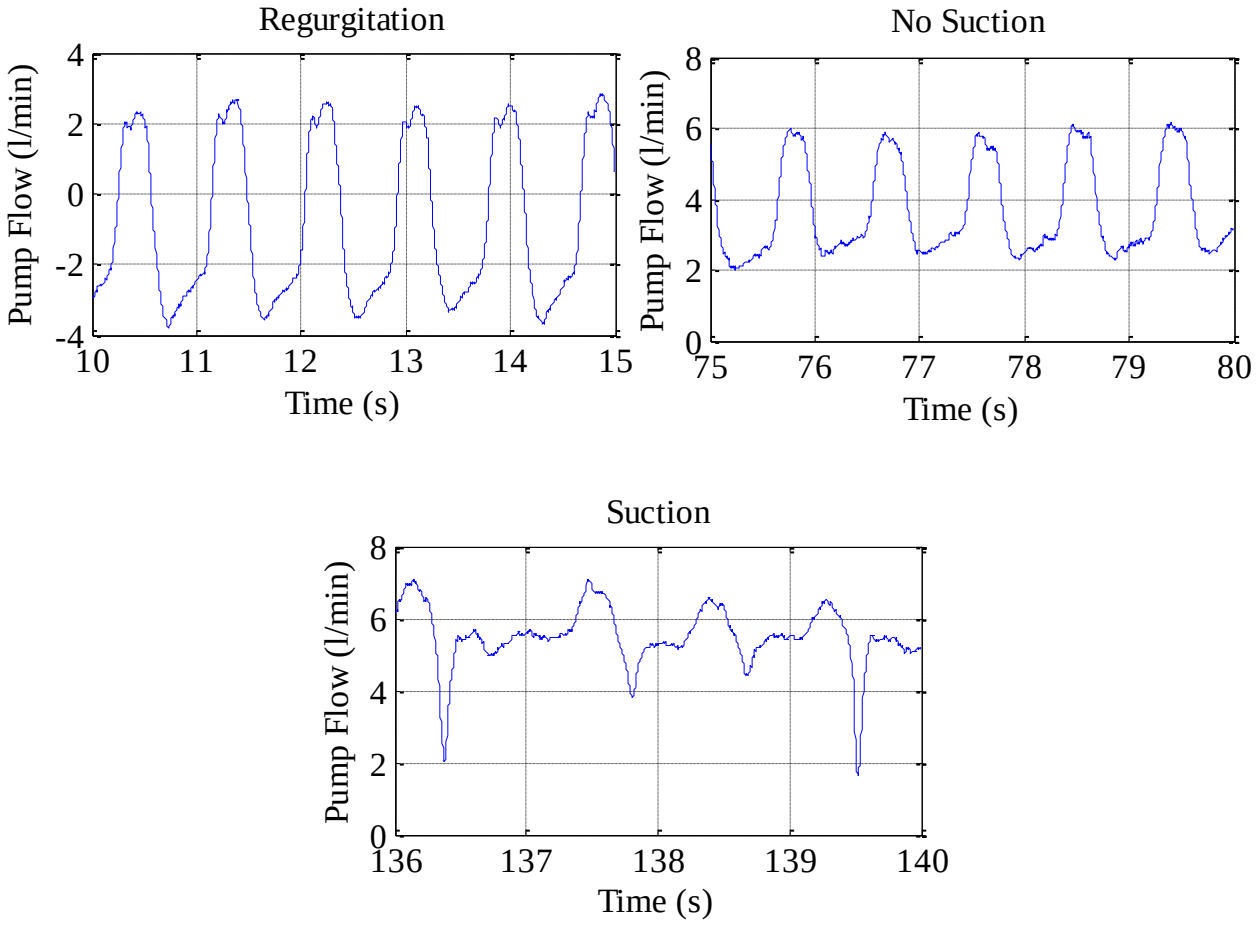

(c)

FIGURE 3.2 Simulation Results in the In-vivo Test

From Figure 3.2, with the pump speed increasing, the amplitude of the pump flow decreases and the envelopes of both maximum and minimum values of the pump flow signal increase gradually. Once the pump speed runs up to a certain value (around 2.7 krpm at 124.6 s), the corresponding pump flow waveform exhibits a sudden large drop in the slope of the envelope of the minimum pump flow signal, indicative of suction, which occurs at 124.6 s < t < 150 s. In addition, under the normal condition (i.e., no suction), the Pump Flow (PF) resembles a sinusoid that can be approximately expressed as follows:

$$PF = a\sin(2\pi ft + \phi) \tag{3.1}$$

However, once suction occurs, the pump flow waveform changes to be asymmetric, varying irregularly that can be easily observed in Figure 3.2 (c) as zoomed plots.

Using the cardiovascular-LVAD model in Chapter 2, similar simulation results can also be obtained compared with these in the in-vivo test. This is shown in Figure 3.3 with different R_S (R_S = 1.0 mmHg.s/ml in (a) and R_S = 1.2 mmHg.s/ml in (b), respectively), and the pump speed is the same as that in Figure 2.13 (a). With these simulation results, if the patient activity level is lower (i.e., an increase in R_S in Figure 3.3 (b)), suction can occur faster compared with the condition of the higher activity level (smaller R_S), and the envelopes of both maximum and minimum pump flow values with smaller R_S are greater than those with larger R_S.

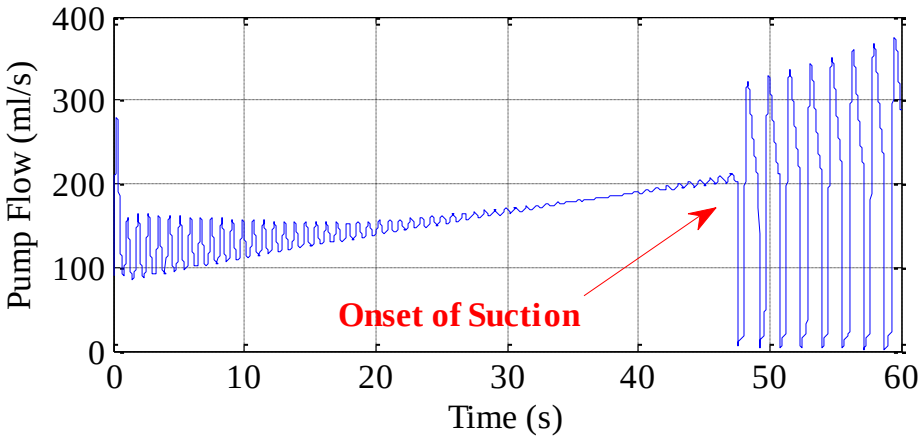

(a)

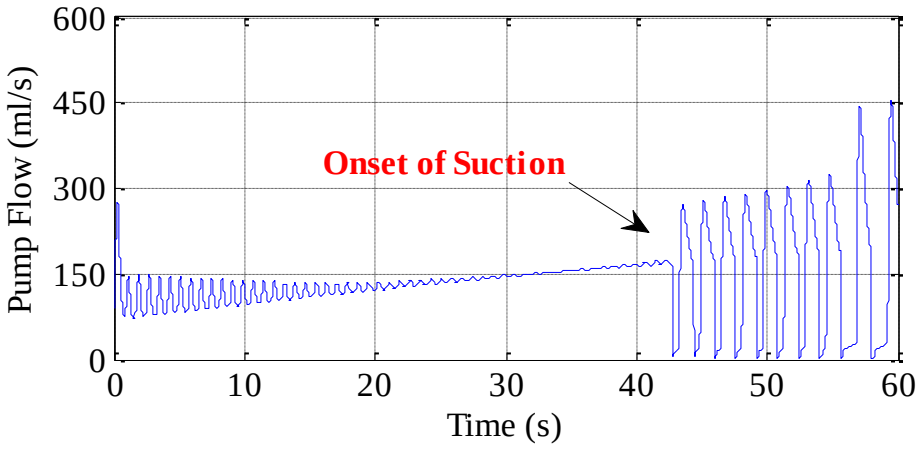

(b)

FIGURE 3.3 Pump Speed with Different Rs with Cardiovascular-LVAD Model Simulation

3.2 Analysis of Suction Indices from Pump Flow

Suction could be easily identified if reliable pressure sensors are implanted at some locations in the left ventricle to continuously measure hemodynamic variables such as x_1 through x_5 (presented in the aforementioned model), or at the inlet of the pump to evaluate the Pump Inlet

Pressure (PIP). Figure 3.4 illustrates the LVP and PIP from in-vivo data with the Nimbus LVAD. The pump speed is the same as shown in Figure 3.2 (a).

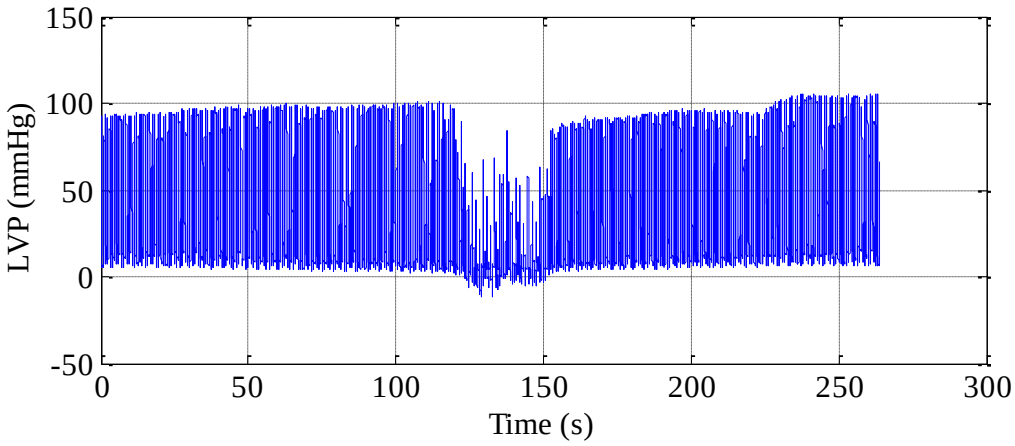

(a)

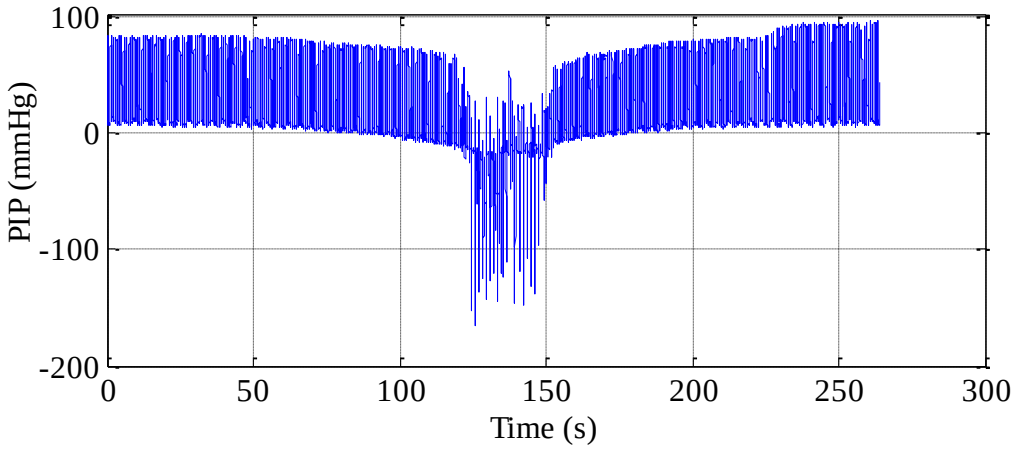

(b)

FIGURE 3.4 In-vivo Simulations

In Figure 3.4, when suction occurs, both LVP and PIP change drastically, meaning that suction can be easily detected if these variables are accurately measured. However, currently such

implantable sensor technology is not available for real-time monitoring. Hence, because of the lack of available information, most suction detection methods are tentative and depend on the extraction of features from other available signals, which can be continuously measured for a long time. Due to these constraints, most researchers use pump flow, pump speed, or pump current to extract features and then detect suction. In this work, the pump flow signal is adopted to extract features.

Features extraction from the pump flow signal in the LVAD has been studied for several years. Several different features from the pump flow have been extracted then used as suction indices to classify the pump flow status. These features are based on different domains (time-domain, frequency-domain, and time-frequency-domain). One of these suction indices is based on the "Mean-Min-Max" criterion [4, 5], which is related to the mean, minimum, and maximum values of the pump flow. Figure 3.5 shows the pump flow and envelopes of mean, minimum, and maximum values of the pump flow with in-vivo data.

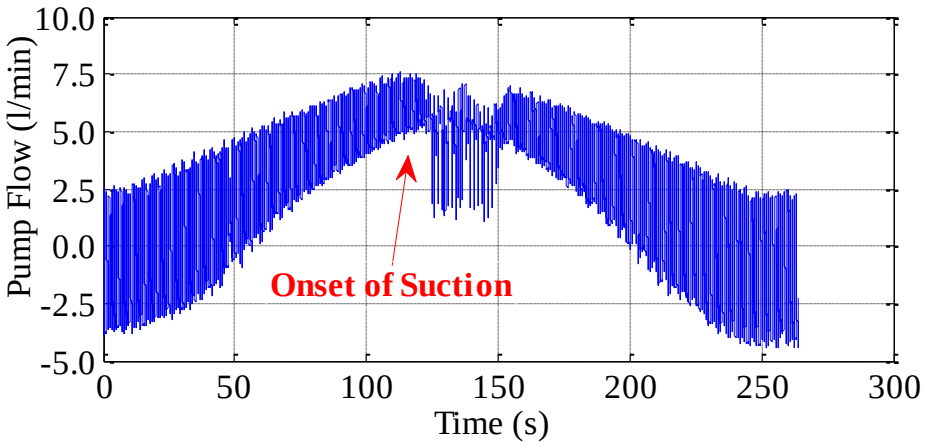

(a)

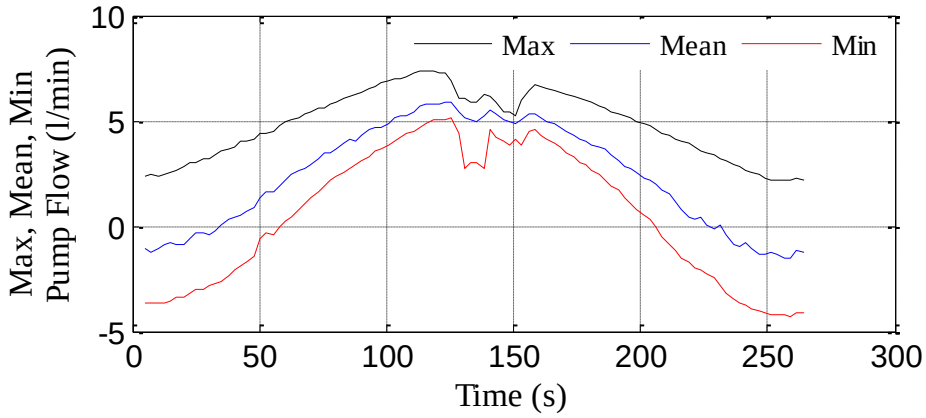

(b)

FIGURE 3.5 Simulation Results of In-vivo Data

Clearly during the suction period (124 s < t < 150 s), the mean value of the pump flow is close to the maximum value of the pump flow, but outside of suction, the mean pump flow value is approximately half of the sum of the maximum and minimum values of the pump flow. Therefore, a time-based index can be derived such that

$$SI = \frac{2mean(PF) - \max(PF) - \min(PF)}{e} \tag{3.2}$$

Where e in equation (3.2) is the peak-to-peak amplitude of the pump flow signal.

The expressions in equations (3.2) [4] can be used as a suction index (SI). The simulation results of it can be implemented in MATLAB; however, the issue of window size needs to be taken into consideration. In fact, window size is a complicated problem for parameters calculation when used to extract features from a given number of samples of the pump flow or other available signals. If the window size is too short, it is helpful to get available information about the pump status faster. However, short window size may not provide meaningful information. Conversely, according to [13], a larger window size may not be feasible in practice while operating the model or system in real-time.

Most researchers developed some approaches to extract features with different-size windows. For instance, Vollkron et al. [4] used a 5-second-long window. Ferreira et al. [13] also adopted a 5-second-long window. Morello [25] presented a 2-second-long window and Karantonis et al [26] used a 6-second-long window. Their window sizes were different but all the experimental results were acceptable. In this thesis, a 5-second-long window is used for the simulations.

Figure 3.6 shows the simulation results of SI with in-vivo data. Under no suction condition, the values of SI do not change largely; instead, it just varies in a small fixed range. But when suction

occurs, SI increases largely; Therefore, this suction index can correctly identify the occurrence of suction in the pump flow around 125 s < t < 150 s.

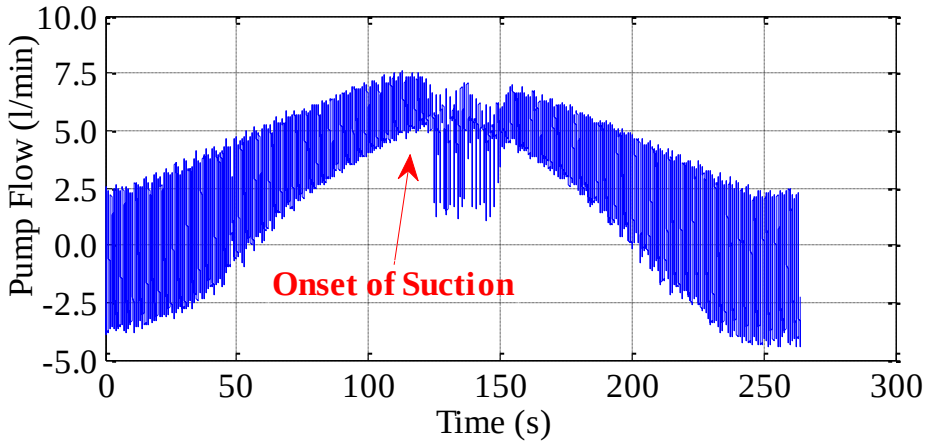

(a)

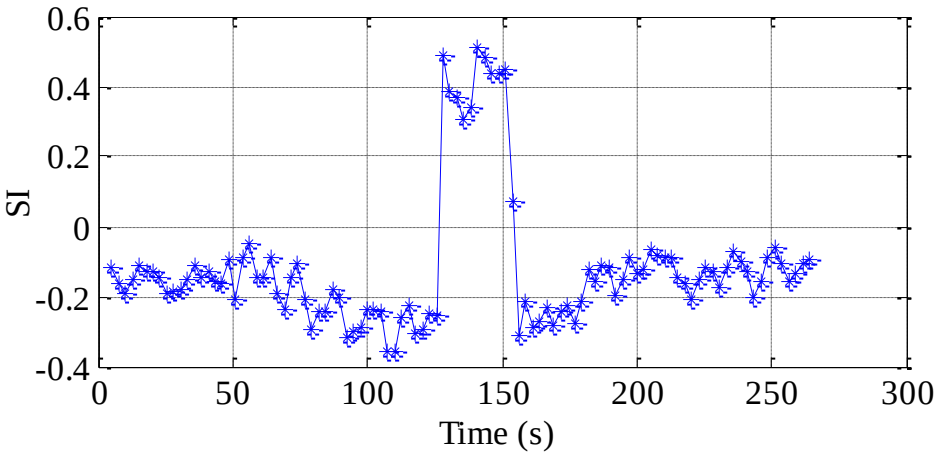

(b)

FIGURE 3.6 Simulation Results of the Time-Based Suction Index

3.3 Simulation with Cardiovascular-LVAD Model

In this section, simulation studies are implemented with the cardiovascular-LVAD model discussed in Section 2.4 instead of the in-vivo test to check the suction detection performance in response to the changes of physiological parameters. Figure 3.7 shows the related block diagram. During this test, E_{max} equals to 1.0 mmHg/ml as simulating a sick heart, and the heart rate is assumed to be constant at 75 bpm. R_S changes from the baseline level of activity (R_S = 1.0 mmHg.s/ml) to the lower level of activity (R_S = 1.2 mmHg.s/ml).

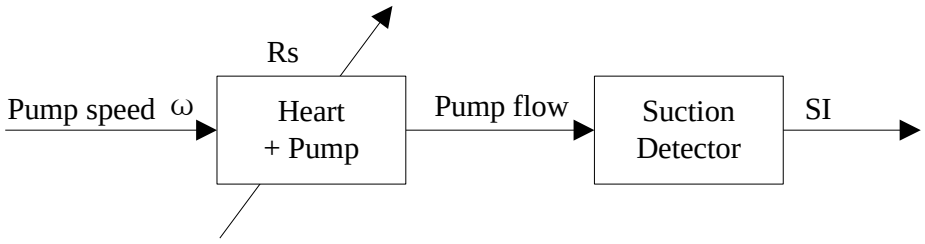

FIGURE 3.7 Block Diagram of Combined Heart + Pump Model and Suction Indicator

R_S, meaning the systemic vascular resistance, represents the afterload in the left ventricle; it varies due to pathological changes of the arteriole in systemic circulation or the vasodilation and vasoconstriction caused by the neurohumour. In cardiovascular physiology, the Systemic Vascular Resistance (SVR) can be expressed with units of dyn.s/cm^5, and its reference range is 900-1400 dyn.s/cm^5 [27]. But if converted to units of mmHg.s/ml, the new reference range is

0.675-1.025 mmHg.s/ml. Hence, in this thesis, the chosen values of R_S in the range of 0.5-1.2 mmHg.s/ml are adequate for the simulations.

Figures 3.8 and 3.9 illustrate the simulation results of SI for a sick heart with different R_S values. From these simulation results, SI increases largely under the suction condition, hence, this suction index can be potentially used as the suction detector for the heart-pump model.

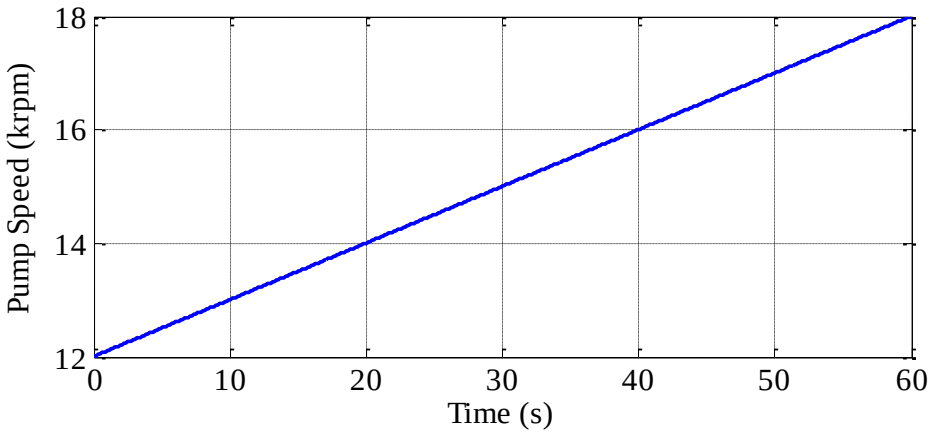

(a)

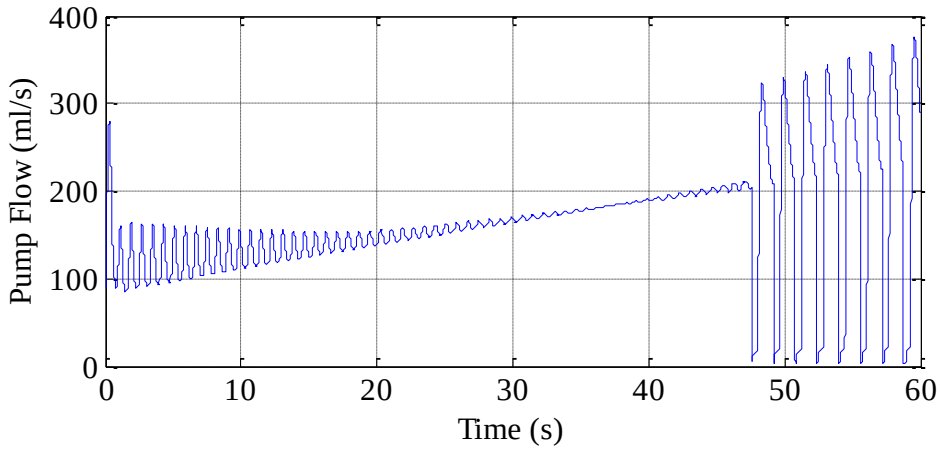

(b)

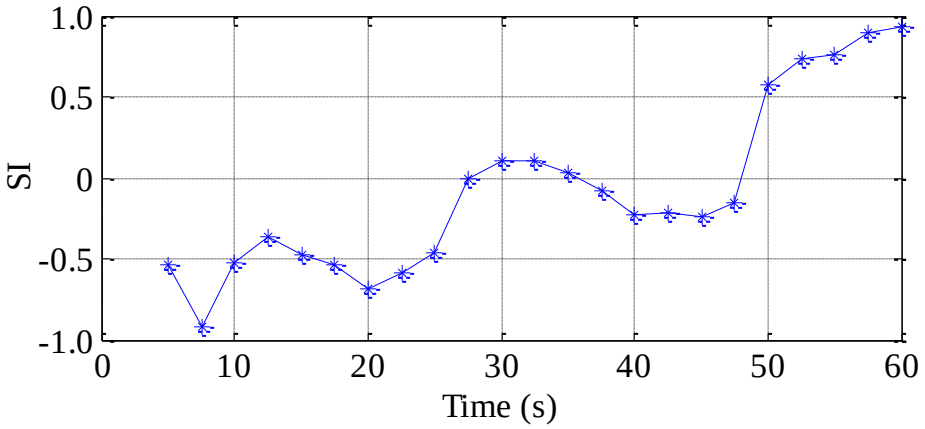

(c)

FIGURE 3.8 Simulation Results of SI (R_S =1.0 mmHg.s/ml) for a Sick Heart

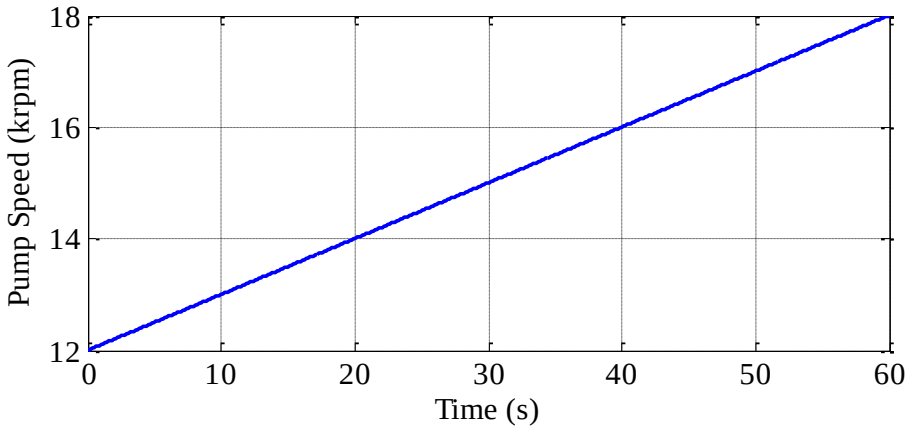

(a)

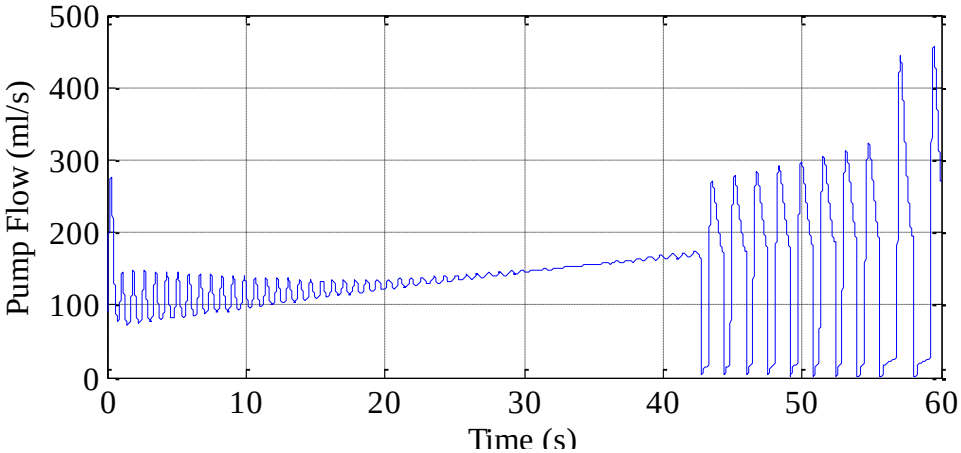

(b)

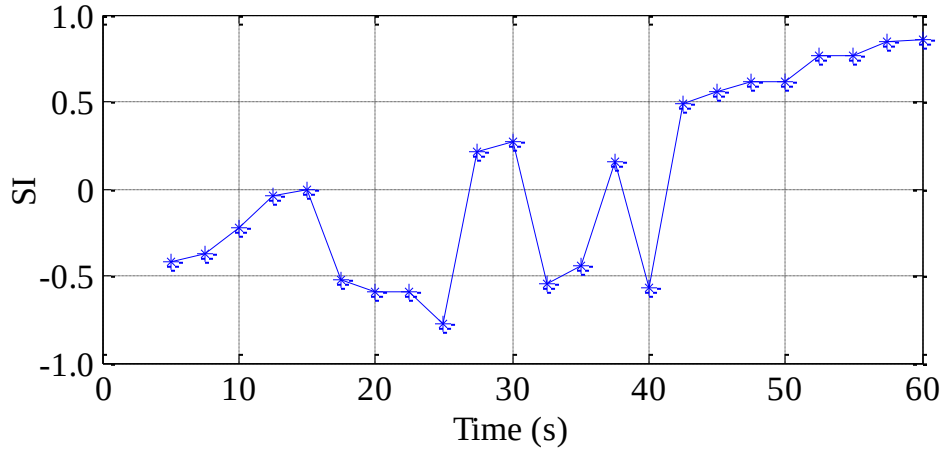

(c)

FIGURE 3.9 Simulation Results of SI (R_S =1.2 mmHg.s/ml) for a Sick Heart

CHAPTER 4:DEVELOPMENT OF A FEEDBACK CONTROLLER FOR LVAD

The objective to develop a feedback controller of rotary Left Ventricular Assist Device (LVAD) is to make the controller automatically adjust the pump speed, the control variable in the system in order to avoid suction and meet the patient's required Cardiac Output (CO) and perfusion pressure (mean arterial pressure), which should be in a normal or acceptable range.

The open-loop operation has been discussed in Chapter 2. However, there is a serious disadvantage such that this operation can be done by the trained technicians or clinicians only. Once such personnel are not present, the patient will be most likely in danger since the pump speed cannot be properly controlled and the situation may be worse when there is a change of the patient activity level. Therefore, the term "automatic adjustment" means the pump speed should be automatically controlled by an appropriate feedback controller according to the changes of the patient different activity levels (i.e., different R_S values).

Therefore, the goal in the thesis is to develop a proper feedback controller in the LVAD to adaptively control the pump speed and at the same time to avoid the occurrence of suction with two constraints such that both cardiac output and mean arterial pressure provided by the LVAD

are sufficient under the patient's physiological conditions. Several proper feedback controllers based on pump flow, pump speed, and pump current with different methods have been proposed.

In this chapter, a new feedback controller for rotary LVAD is presented. The suction index described in Chapter 3 is extracted from the pump flow signal and used as the input of the feedback controller. A threshold is set according to the value of the suction index. The constant threshold is used to compare with the suction index to determine how to continuously update the pump speed.

This chapter is organized as follows. Section 4.1 describes the development of the feedback controller. Section 4.2 shows the simulation results in details, including checking the performance of this proposed controller and assessing whether the cardiac output and perfusion pressure generated by the controller are acceptable compared with the reference values. The robustness of the controller to measurement noise at different signal-to-noise ratio (SNR) levels is also discussed.

4.1 Development of A Feedback Controller

To develop a proper feedback controller, a threshold is presented. By comparing the threshold with the suction index, the pump speed can be correctly updated such that if the value of the suction index is no more than that of the threshold, the pump speed will increase, otherwise the

pump speed will decrease, which is the rule for the pump speed update. Figure 4.1 shows the block diagram of the developed feedback controller for the rotary LVAD.

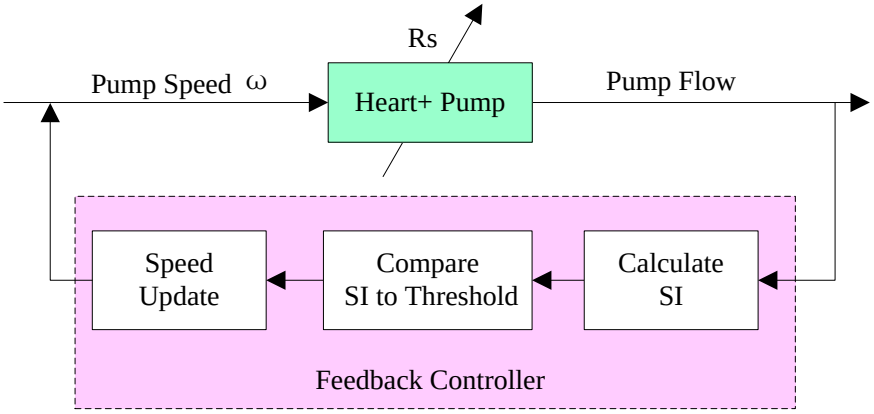

FIGURE 4.1 Block Diagram of Proposed Controller

From Figure 4.1, the entire control system consists of two parts. First, after measuring the pump flow in the cardiovascular-LVAD model, the Suction Index (SI) can be calculated with equation (3.3). In this part, the mean, minimum, and maximum values of the pump flow signal within every cardiac cycle need to be tracked. A moving window consisting of a number of past values of mean, minimum, maximum values of the pump flow signal is used. Second, a constant threshold is used as part of the feedback controller to compare with the calculated SI in order to continuously update the pump speed using the update rule previously discussed. The updated pump speed is as follows:

$$\omega(k+1) = \omega(k) + acb \tag{4.1}$$

Where k is the update sample, c is the constant adjustment parameter and b is the absolute value of the mean pump flow signal at current sample. The parameter "a" is represented by the following expression

$$a = \begin{cases} 1, & if\ SI \le threshold \\ -1, & if\ SI > threshold \end{cases} \tag{4.2}$$

Note that the choice of the threshold is crucial and its effect may be sensitive; it needs to be chosen according to the suction index. If the threshold value is much larger than the suction index value, the pump speed has to increase until the most recent value of the suction index is no less than that of the threshold. As a result, suction may occur since the increasing pump speed can be out of the suction speed (the speed when suction occurs). Correspondingly, "backflow" may also occur if a smaller threshold value is chosen. Figure 4.2 shows the flow chart for updating the pump speed.

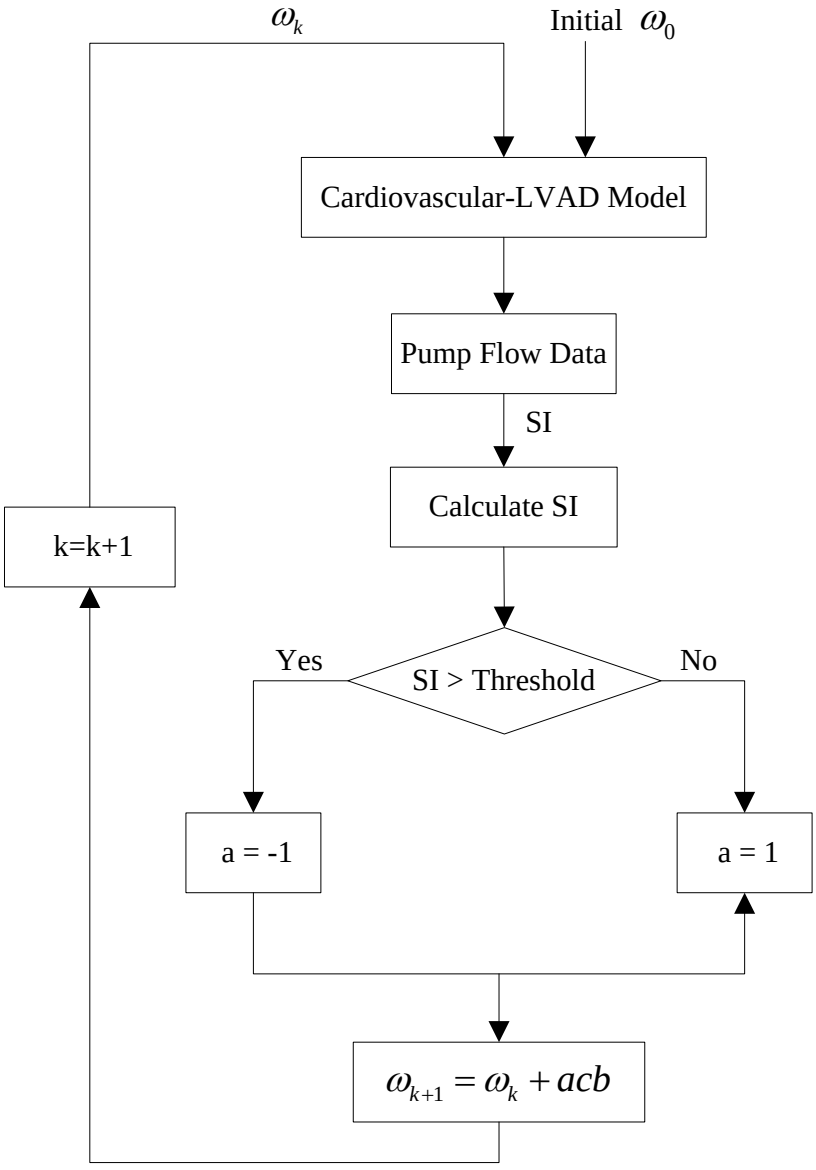

FIGURE 4.2 Flow Chart for Updating Pump Speed

4.2 Simulation Studies

In this section, simulation studies are implemented in MATLAB to evaluate the performance of the proposed feedback controller with an initial ramp pump speed and the patient different activity levels, and then check the actual cardiac output, perfusion pressure generated by the controller and robustness of the controller to measurement noise. The reason why the simulations are carried out is that for the animal in-vivo test, it is difficult to implement varying physiologic parameters compared with the simulation methods that can deal with the changes of such parameters.

In order to prove the effectiveness of this proposed feedback controller, the cardiovascular-LVAD model shown in Figure 2.11 is used. In all the simulations, we set E_{max} = 1.0 mmHg/ml, representing a sick heart. In addition, the heart rate is set as constant at 75bpm and the value of threshold is 0. The adjustment parameter is 0.05. A continuously moving window is also used with a step size of 0.01 s. Furthermore, there are two approaches to initialize the pump speed: set it low or high at the beginning. However, initializing a high pump speed is not feasible for patients since it is most likely to cause suction. Hence, the initial pump speed is set at 13000 rpm and linearly increases with the slope of 50. After the first 2.4 s, the controller starts taking action.

4.2.1 Simulation with A Sick Heart

In this section, all the simulations are implemented with both constant Systemic Vascular Resistance (SVR) and changing SVR values. Furthermore, the related hemodynamic analysis for cardiac output and mean arterial pressure is discussed.

4.2.1.1 Constant Systemic Vascular Resistance

Constant SVR indicates a patient whose level of activity is not changed for a period of time. In this simulation, we set R_S = 1.0 mmHg.s/ml, under this condition suction occurs at around 46 s with ω = 16600 rpm. Fig. 4.3 (a) shows Pump Speed versus time as generated by this proposed feedback controller and Fig. 4.3 (b) shows the corresponding Pump Flow signal versus time. In this figure, the controller is able to increase and decrease the pump speed in a fixed range but definitely below the suction speed. The reason that the pump speed is always fluctuating and cannot be greater than the suction speed is due to the threshold preset to restrict the pump speed.

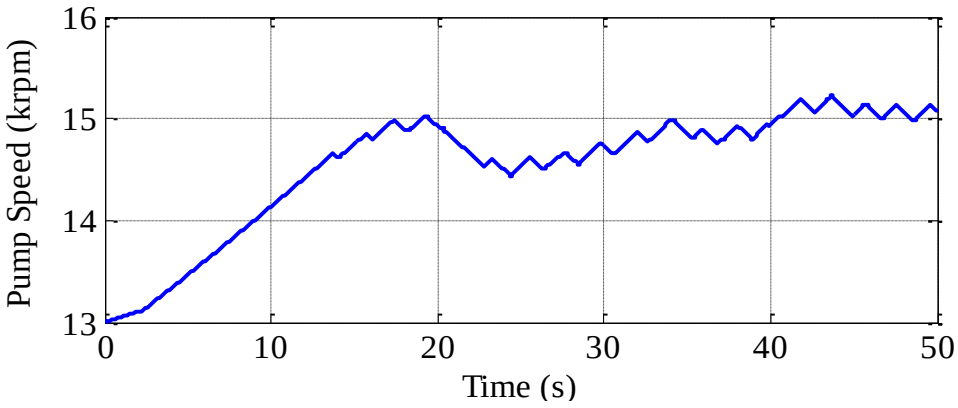

(a)

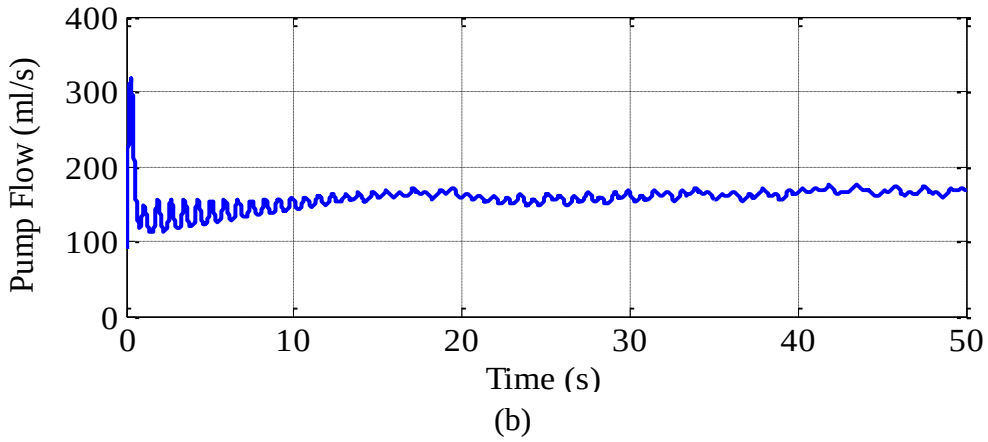

(b)

FIGURE 4.3 Simulation Results with Constant Rs

4.2.1.2 Changing Systemic Vascular Resistance

To mimic a condition of a time-varying activity level of a heart failure patient, R_S is set in equation (4.3) and Figure 4.4 as follows:

$$Rs = \begin{cases} 0.5, & if \ \ 0 \le t \le 20 \\ 0.5 + 7(t-20)/100, & if \ \ 20 \le t \le 30 \\ 1.2 & if \ \ 30 \le t \le 50 \end{cases} \tag{4.3}$$

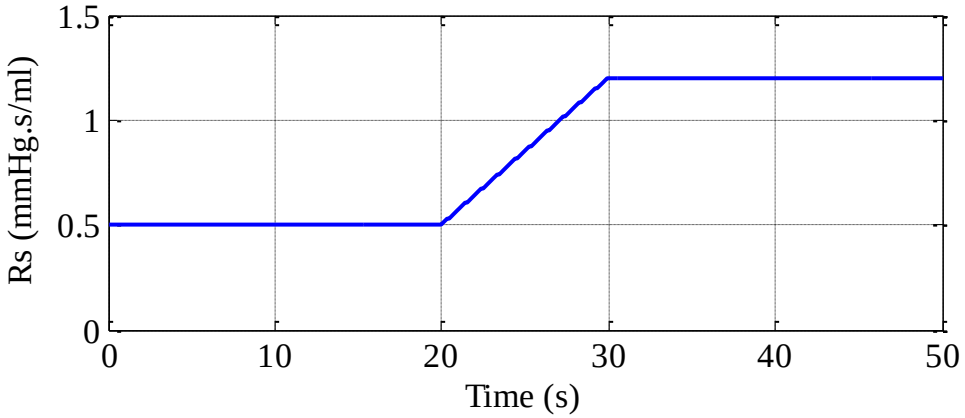

FIGURE 4.4 Changing Systemic Vascular Resistance

Note that the suction speed will vary according to the changing SVR values. When R_S equals to 0.5 mmHg.s/ml, the suction speed is 19000 rpm, which decreases to 16100 rpm with R_S equals to 1.2 mmHg.s/ml. Fig.4.5 (a) is the response to the pump speed and the related pump flow signal is shown in Fig. 4.5 (b). Clearly, the controller is still able to adjust the pump speed in a fixed range to avoid suction although under the condition of varying SVR.

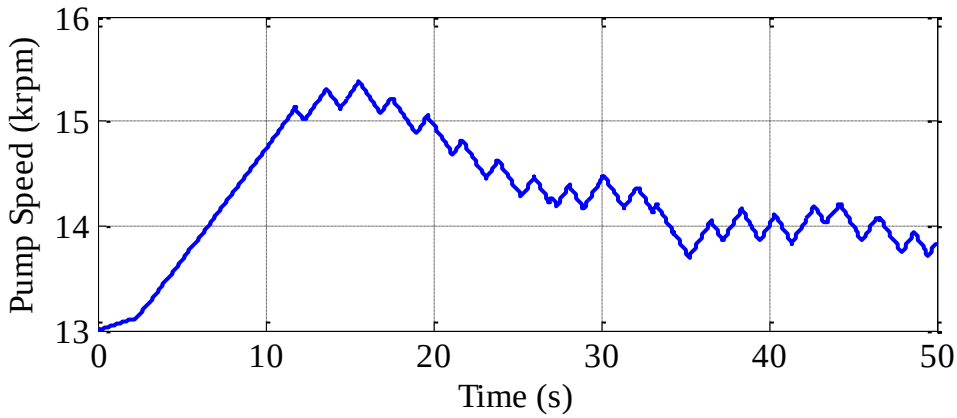

(a) Pump Speed

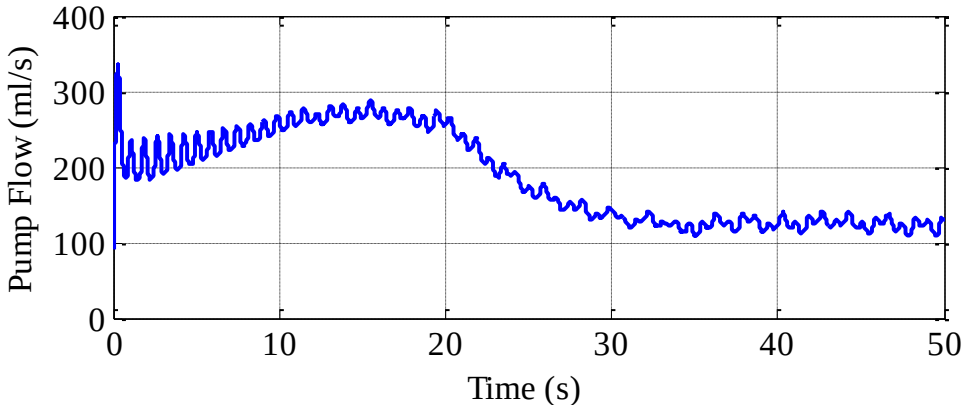

(b) Pump Flow

FIGURE 4.5 Simulation Results with Changing R_S

4.2.2 Hemodynamic Analysis

In this research, in addition to avoiding suction, another main objective of developing a feedback controller for the LVAD is to make sure that the Cardiac Output (CO) and Mean Arterial Pressure (MAP) generated by the controller can meet the body's normal requirements for patients with congestive heart failure. For a healthy heart, the cardiac output can be easily calculated based on equation (2.2), however, for a sick heart with the LVAD, equation (2.2) will not be available since with the LVAD the sick heart is taken over by the rotary pump that can produce needed cardiac output to support the sick heart. As a result, the actual cardiac output with the LVAD is the summation of the blood flow pumped by the heart and the pump flow through the LVAD. In addition, in Figure 2.13 (b) in Chapter 2, as previously discussed, AoP is always larger than LVP, which means due to the weak contractility of the sick heart, the LVAD can provide 100% of the cardiac output, therefore, the cardiac output is equal to the pump flow.

In cardiovascular physiology, pressure is produced as blood is pumped out of the left ventricle into the artery [28], and the Mean Arterial Pressure (MAP) is considered as the perfusion pressure. In real-time, MAP can be approximately calculated with the more easily measured systolic and diastolic pressures as follows [29]:

$$MAP \approx DP + \frac{1}{3}(SP - DP) \tag{4.4}$$

Or equivalently

$$MAP \approx \frac{1}{3}(2DP + SP) \tag{4.5}$$

Or equivalently

$$MAP \approx \frac{2}{3}DP + \frac{1}{3}SP \tag{4.6}$$

Or equivalently

$$MAP = DP + \frac{1}{3}PP \tag{4.7}$$

Where DP is the diastolic pressure, SP is the systolic pressure, PP is the pulse pressure that equals to the difference between SP and DP. However, these four expressions in equations (4.4)~(4.7) are only available at a normal resting heart rate. At a high heart rate, MAP is more closely calculated by the arithmetic average of the systolic pressure and diastolic pressure due to the change in the shape of the arterial pressure pulse [28]. Therefore, a general expression for calculating MAP is expressed as follows [28]:

$$MAP = CO * SVR + CVP \tag{4.8}$$

Where CVP is the central venous pressure. In equation (4.8), the Mean Arterial Pressure (MAP) is determined by Cardiac Output (CO), Systemic Vascular Resistance (SVR), and Central Venous Pressure (CVP). Figure 4.6 shows their relationship.

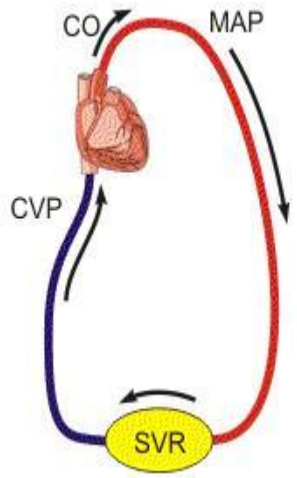

FIGURE 4.6 Relationship between MAP, CO, SVR, and CVP [28]

Furthermore, the value of CVP is usually very small, which often can be neglected. However, to express MAP as precise as possible, in this work CVP is taken into consideration when calculating MAP. Actually CVP is not only small (several mmHg even near 0 mmHg), but also time-varying. Figure 4.7 illustrates CVP related to the pump flow in Figure 3.2 (i.e., suction occurs around 125 s < t < 150 s).

In Figure 4.7, outside of suction the mean value of CVP is 11.3 mmHg, which is around 12 mmHg under the suction condition. Since suction needs to be avoided, in this research CVP

equals to 11.3 mmHg is used in equation (4.8). Notice that in general, all the values of CVP from 0 mmHg to 15 mmHg that is the maximum value outside of suction in Figure 4.7 are acceptable.

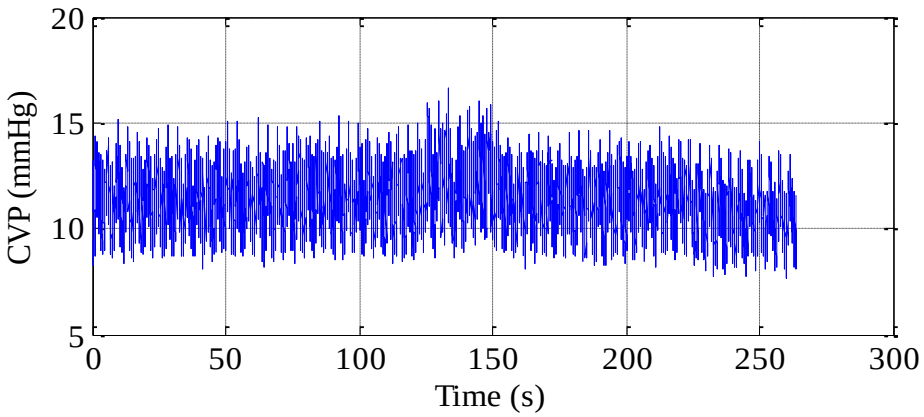

FIGURE 4.7 Central Venous Pressures with In-vivo Data

To prove the effectiveness of equation (4.8) in this work, two different tests with and without the LVAD are implemented. Figure 4.8 illustrates the comparison between the measured MAP using the model as a healthy heart (i.e., without the LVAD) in Figure 2.7 and the calculated MAP with equation (4.8). Under the baseline condition (R_S = 1.0 mmHg.s/ml), the measured value of MAP is 91.24 mmHg, the calculated MAP is 90.3 mmHg, hence the error is 1%. In the exercise level (R_S = 0.5 mmHg.s/ml) the value of reference MAP is 71.5 mmHg compared with 71.6 mmHg, the calculated value of MAP, representing only a 0.14% error. Under the rest condition (R_S = 1.2 mmHg.s/ml), the measured value of MAP is 94.5 mmHg and the calculated MAP value is 94.6 mmHg, hence the error is only 0.1%.

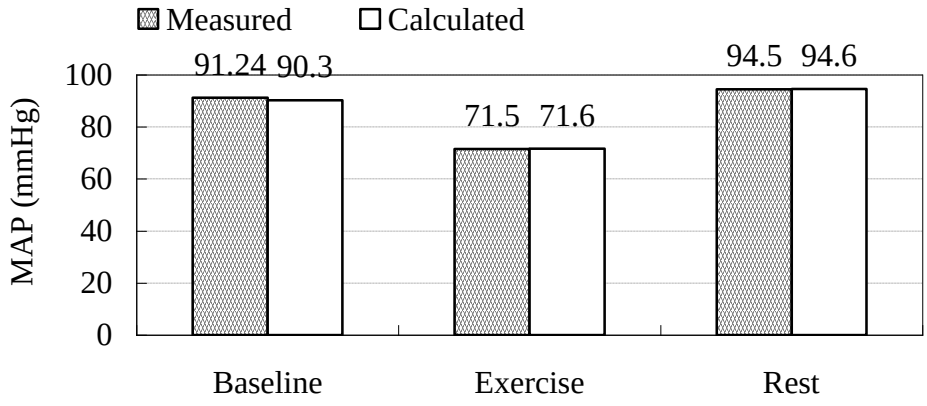

FIGURE 4.8 Comparison between Measured and Calculated MAP

Figure 4.9 shows another comparison between MAP measured in [13] with the LVAD and that calculated by equation (4.8), respectively. With CO equals to 7.0 l/min, the measured value of MAP is 128 mmHg, the same as calculated. When CO is 7.8 l/min the correspondingly measured MAP value is 118 mmHg compared with 115.3 mmHg, the calculated MAP, representing a 2.3% error. With CO equals to 11.0 l/min, the value of MAP measured is 127 mmHg and the calculated value of MAP is 121.3 mmHg, with the error of 4.5%. Therefore, in both Figures 4.8 and 4.9, all the calculated results based on equation (4.8) are acceptable.

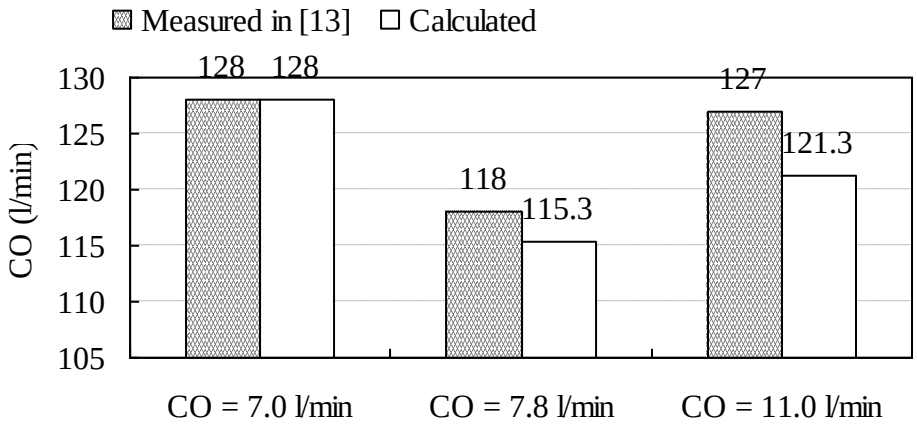

FIGURE 4.9 Comparison between Measured in [13] and Calculated MAP

Figure 4.10 (a) illustrates the results of CO according to the pump flow in Figures 4.3 (b) and 4.5 (b) under the patient different activity levels. Under the baseline condition, the reference COs are 3.8 l/min (as a sick heart without the LVAD) and 4.7 l/min (as a healthy heart without the LVAD), respectively; the proposed controller is able to increase CO to 9.12 l/min for a sick heart. Under the exercise condition, the reference values are 5.6 l/min (sick heart) and 7.2 l/min (healthy heart), respectively; in this case the actual CO with the LVAD is increased to 13.7 l/min. Finally in the rest level, the CO reference values are 3.4 l/min (sick heart) and 4.2 l/min (healthy heart), respectively, and the controller can support 7.5 l/min for a sick heart.

Correspondingly, Figure 4.10 (b) compares the MAP values with varying SVR values from the exercise to the rest level. In the baseline level, the reference MAPs are 75.2 mmHg (as a sick heart) and 90.3 mmHg (as a healthy heart), respectively; the controller generates 163 mmHg for

a sick heart. When the patient is exercising, the reference values of MAP are 59 mmHg (sick heart) and 71.6 mmHg (healthy heart), respectively, and the actual value of MAP with the LVAD is 134 mmHg. In the rest level, the MAP reference values are 77.3 mmHg (sick heart) and 94.6 mmHg (healthy heart), respectively, and the controller provides 161 mmHg for a sick heart.

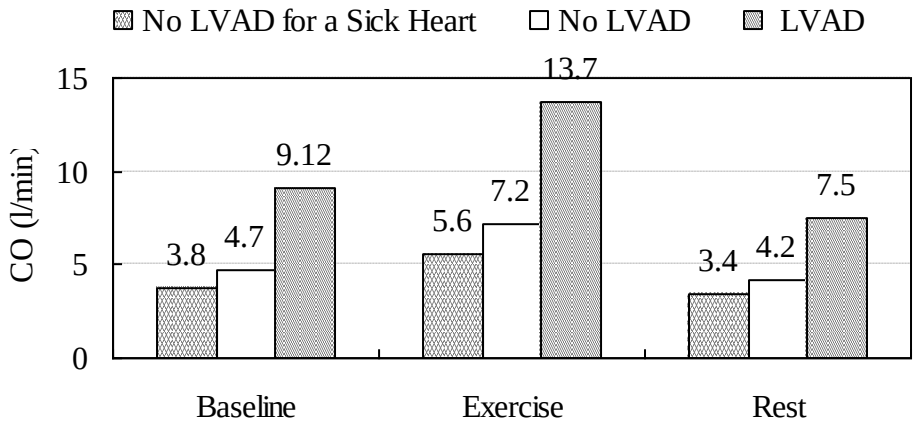

(a) Cardiac Output

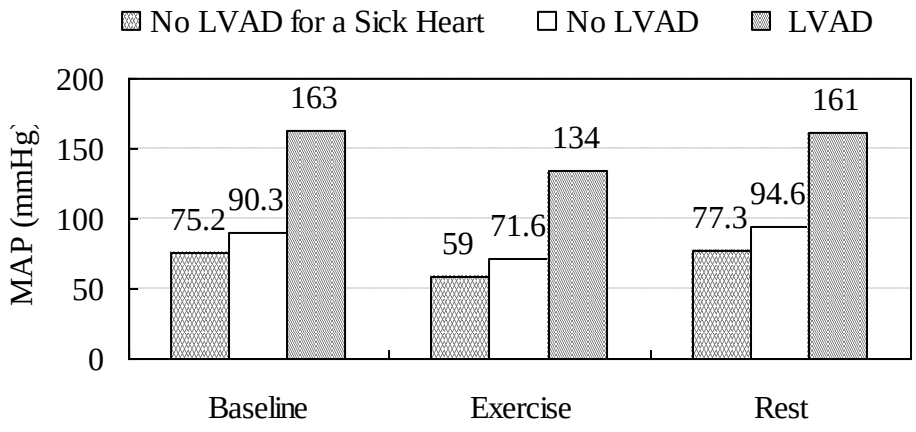

(b) Mean Arterial Pressure

FIGURE 4.10 Hemodynamic Variables Results without and with LVAD

In conclusion, this proposed controller can be able to provide larger cardiac output and mean arterial pressure for a sick heart with the LVAD than these generated by a healthy heart. Moreover, notice that for this control system, as previously mentioned, the cardiac output is equal to the pump flow with the LVAD supporting, hence the mean arterial pressure values obtained are actually based on the pump flow signals.

4.2.3 Robustness to Noise

In this research, the proposed feedback controller relies on only one state variable (the pump flow); therefore, it is important to check its performance when a noisy pump flow signal is present. Simulation studies with uniformly distributed random measurement noise added to the pump flow signal are performed. The objective here is to determine at what level of the signal-to-noise ratio (SNR) the controller can still be able to actuate the pump speed into an acceptable range. To do this, two previous simulations in Section 4.2.1 are repeated with the following four different values of SNR: 30, 20, 10, and 5dB. Moreover, after simulations with each SNR value, the results of related CO and MAP are also discussed. Note that the actual pump flow signal used to calculate SI and CO is with noise.

4.2.3.1 Simulation Results With SNR = 30 dB

Figures 4.11 and 4.12 illustrate the simulation results with uniformly distributed random noise at SNR = 30 dB for constant and changing SVR values, respectively. In both Figures 4.11 (a) and 4.12 (a), the pump speed signals change more frequently than these without noise. For constant SVR, there exist more fluctuations in the pump speed before 15 s, for changing SVR, the pump speed signals vary more frequently until 35 s. However, suction does not occur by observing the net pump flow (i.e., the pump flow without noise) in Figures 4.11 (b) and 4.12 (b). Furthermore, due to the high SNR (30 dB), the actual pump flow signals with noise in Figures 4.11 (c) and 4.12 (c) are similar to the corresponding net pump flow signals in Figures 4.11(b) and 4.12(b), meaning that at SNR = 30 dB, the controller cannot be adversely affected by noise and still works fairly well.

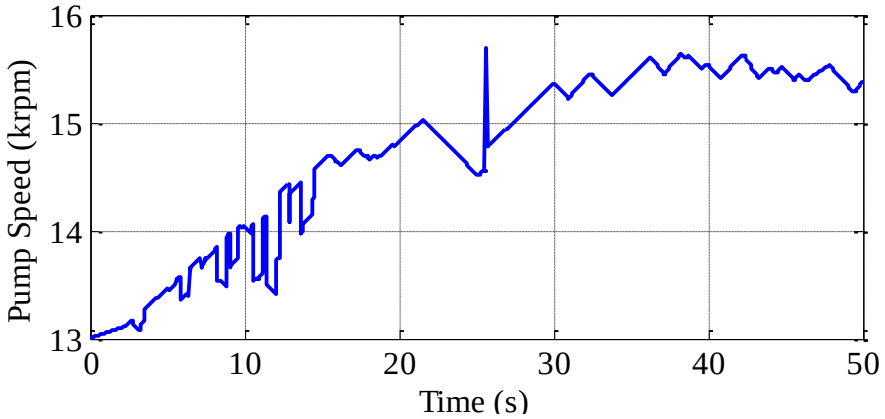

(a) Pump Speed

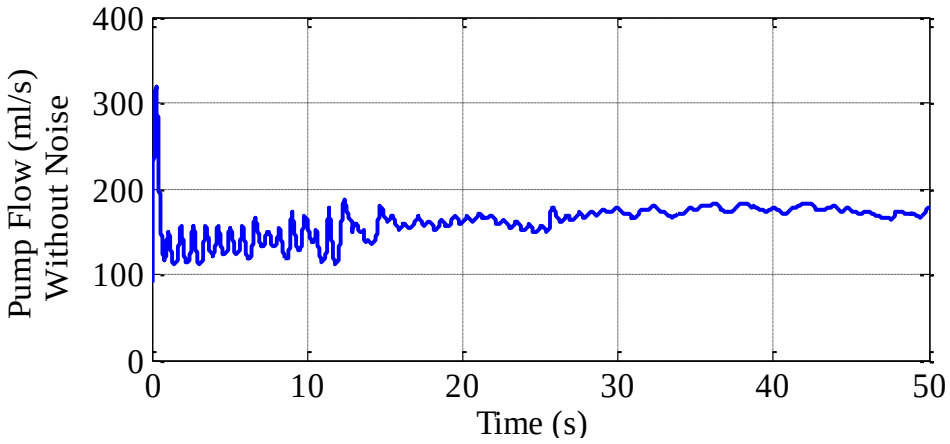

(b) Pump Flow without Noise

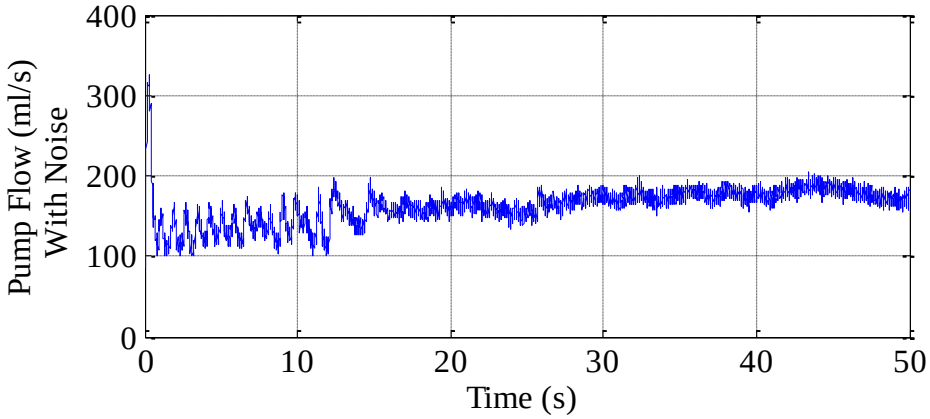

(c) Pump Flow with Noise

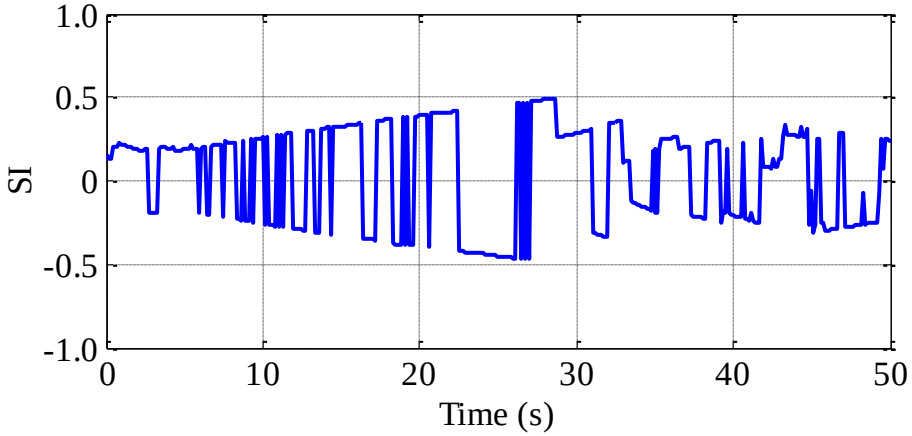

(d) Calculated SI

FIGURE 4.11 Simulation Results of Constant SVR with SNR = 30 dB

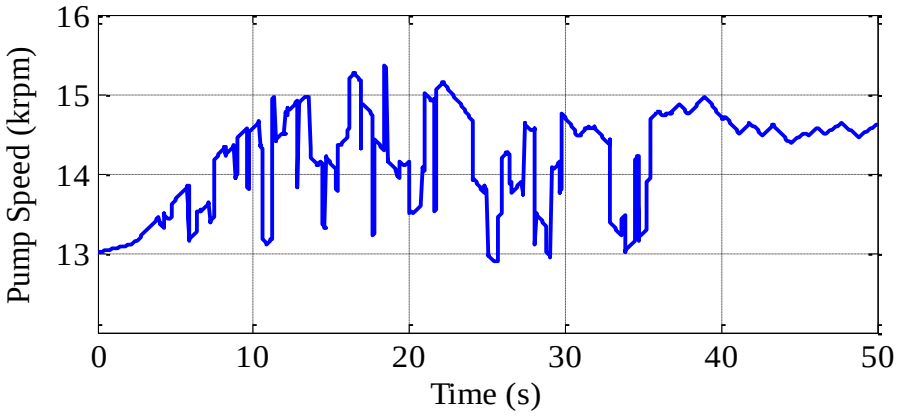

(a) Pump Speed

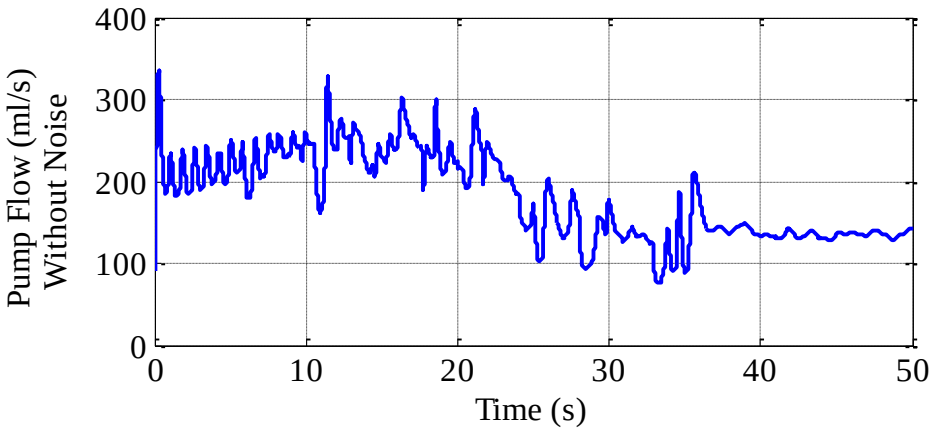

(b) Pump Flow without Noise

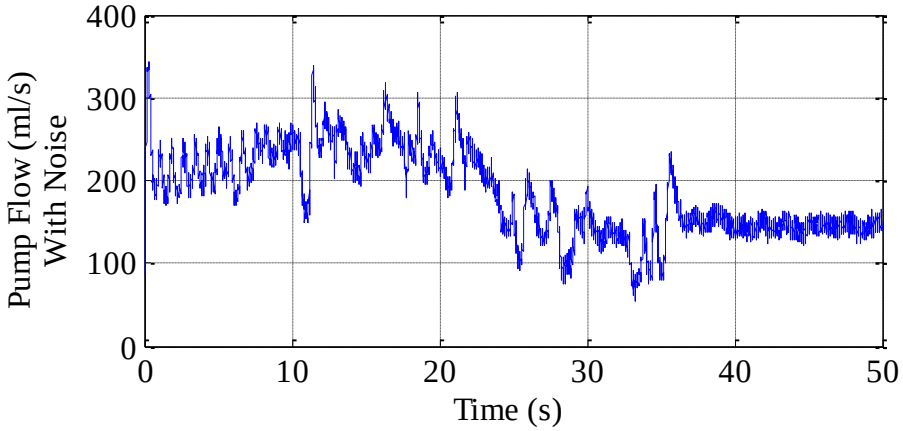

(c) Pump Flow with Noise

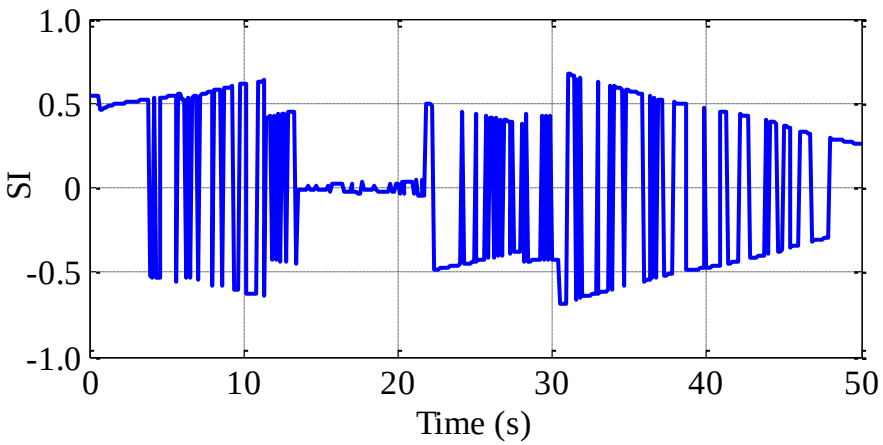

(d) Calculated SI

FIGURE 4.12 Simulation Results of Changing SVR with SNR = 30 dB

Figure 4.13 (a) and (b) shows the comparison of hemodynamic parameters, CO in (a) and MAP in (b) without noise measured in Figure 4.10 (a) and (b) in Section 4.2.2 and these measured with SNR = 30 dB. Notice that in practice the available pump flow includes noise; hence all the measurements should depend on that instead of the net pump flow. Under the baseline condition, CO and MAP without noise are 9.12 l/min and 163mmHg, respectively. With noise adding, the proposed controller generates 9.32 l/min for CO and 173 mmHg for MAP. In the exercise level, without noise CO is 13.7 l/min and MAP is 134mmHg, when there exists noise, the actual CO is 13.3 l/min, the corresponding MAP is 128 mmHg. When the patient is having a rest, the CO value is 7.5 l/min and the measured MAP is 161 mmHg, after adding noise, the two values increase to 7.9 l/min and 170 mmHg, respectively.

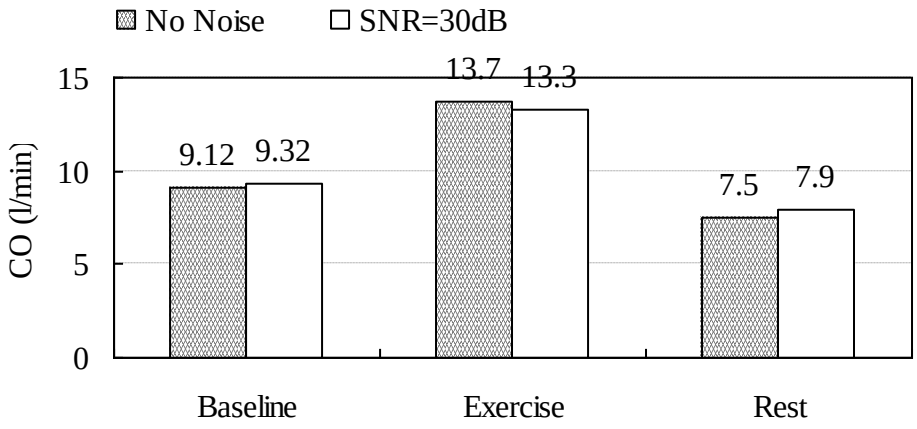

(a) Cardiac Output

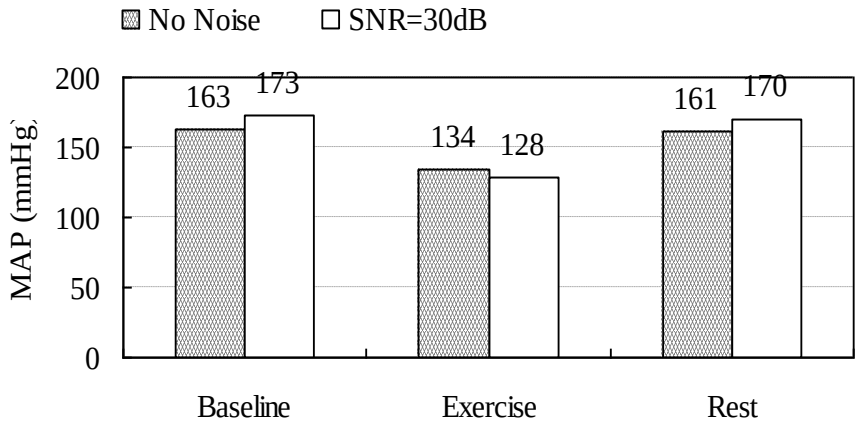

(b) Mean Arterial Pressure

FIGURE 4.13 Hemodynamic Variables Comparison without Noise and with SNR = 30 dB

4.2.3.2 Simulation Results With SNR = 20 dB

With SNR decreasing to 20 dB, Figures 4.14 and 4.15 illustrate the simulation results under constant and changing SVR values, respectively. Similar to the results with SNR = 30 dB, in both Figures 4.14 (a) and 4.15 (a), there still exist frequent changes in the pump speed signals

compared with these without noise. In addition, suction still does not occur since there is not any phenomenon of suction according to the net pump flow signals in Figures 4.14 (b) and 4.15 (b), and the actual pump flow signals with noise in Figures 4.14 (c) and 4.15 (c) are still similar to these without noise, but not as clear as those with SNR = 30 dB due to the lower SNR (i.e., higher noise level) at this time. In summary, the LVAD can still support a sick heart well.

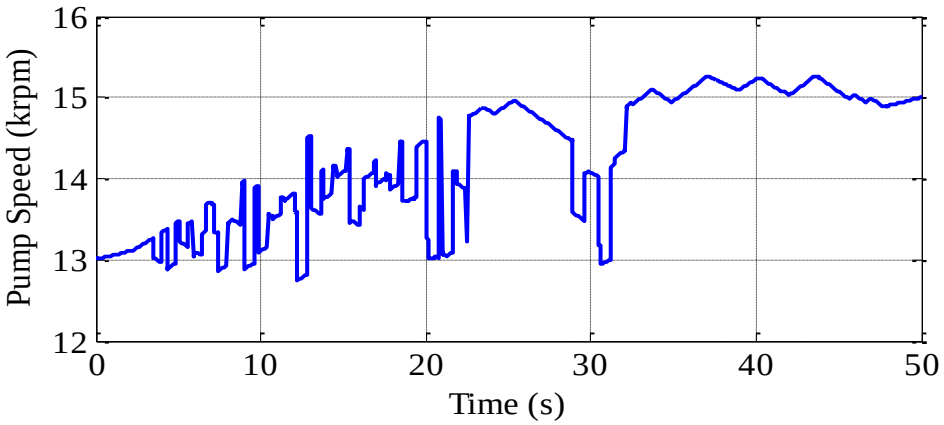

(a) Pump Speed

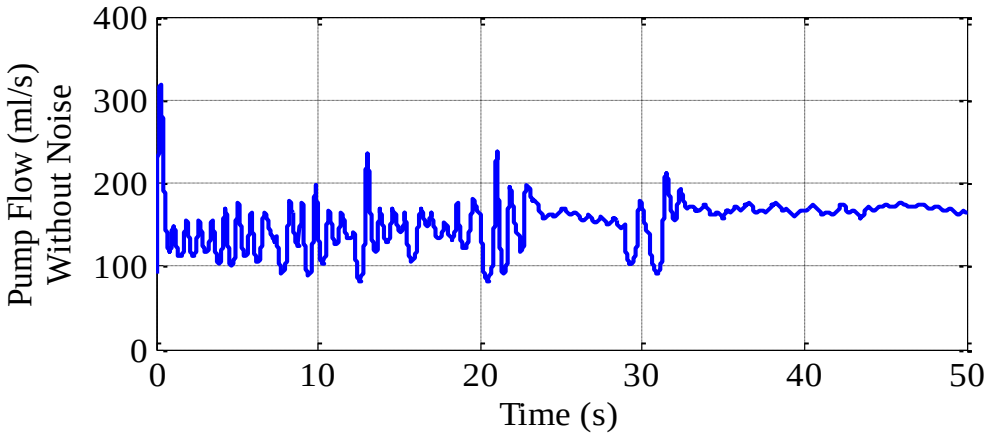

(b) Pump Flow without Noise

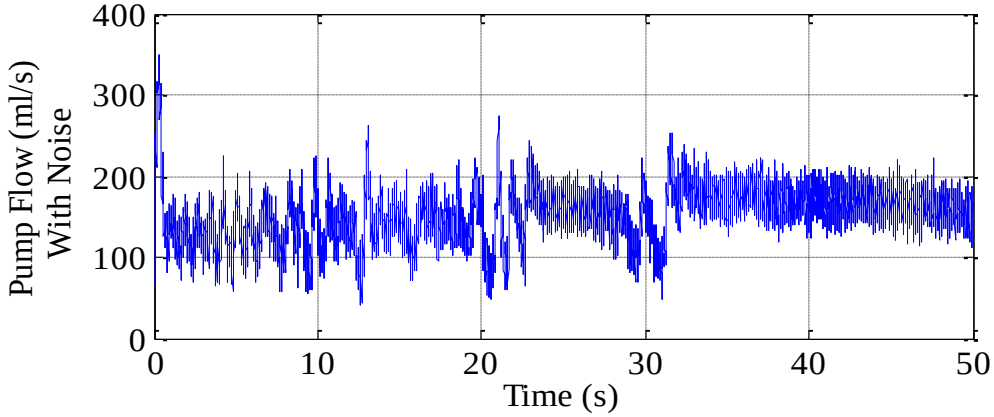

(c) Pump Flow with Noise

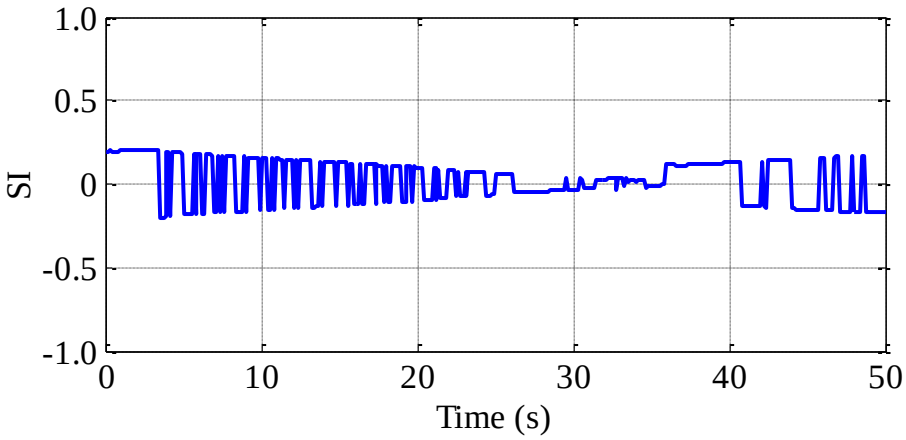

(d) Calculated SI

FIGURE 4.14 Simulation Results of Constant SVR with SNR = 20 dB

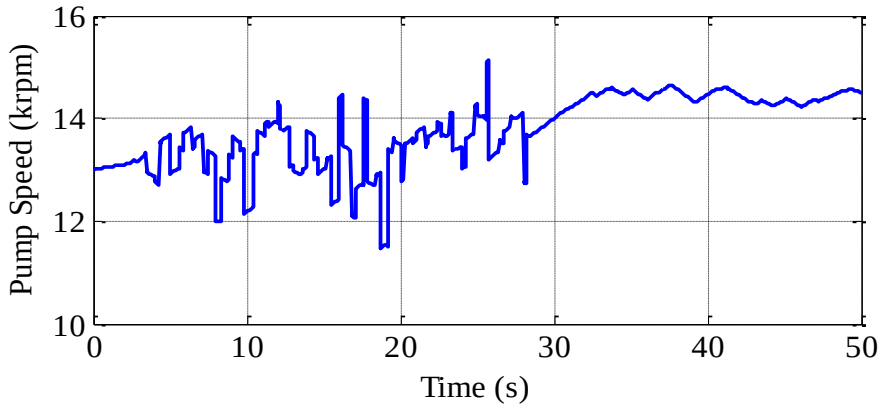

(a) Pump Speed

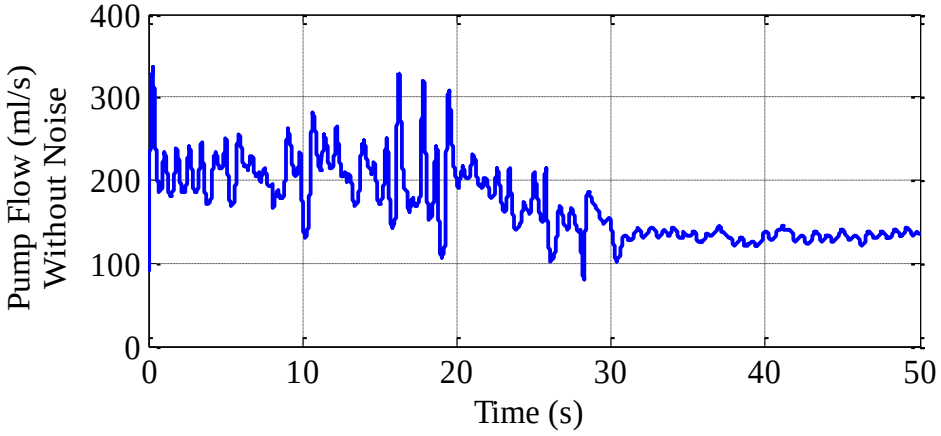

(b) Pump Flow without Noise

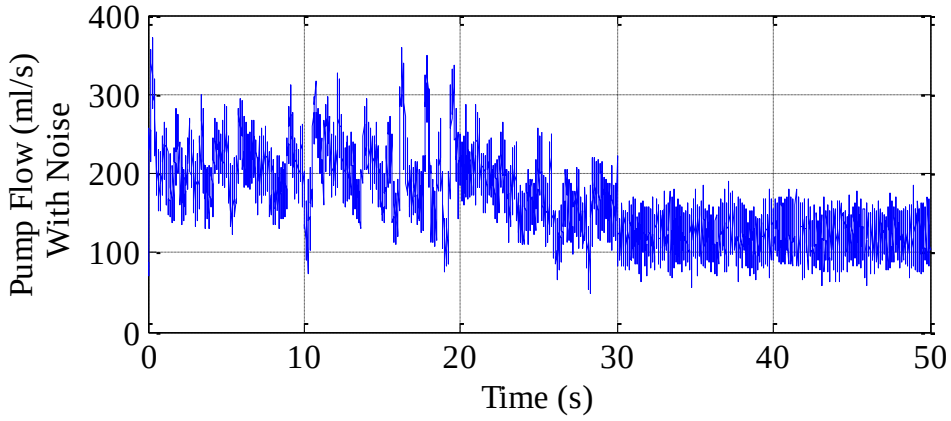

(c) Pump Flow with Noise

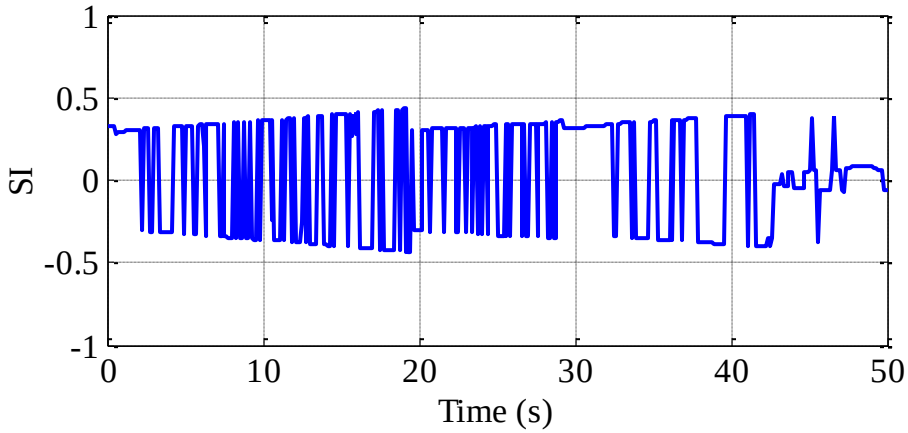

(d) Calculated SI

FIGURE 4.15 Simulation Results of Changing SVR with SNR = 20 dB

The measured CO and MAP based on the actual pump flow with SNR = 20 dB and the corresponding results without noise are shown in Figure 4.16 (a) and (b), respectively. At this time the values of CO reduce to 9.18 l/min, 12.6 l/min, and 7.32 l/min compared with the related values with SNR = 30 dB under the baseline, exercise, and rest conditions, respectively. The values of MAP decrease to 164 mmHg, 116 mmHg, and 158 mmHg with R_S equals to 1.0, 0.5, and 1.2 mmHg.s/ml compared with the results at SNR = 30 dB.

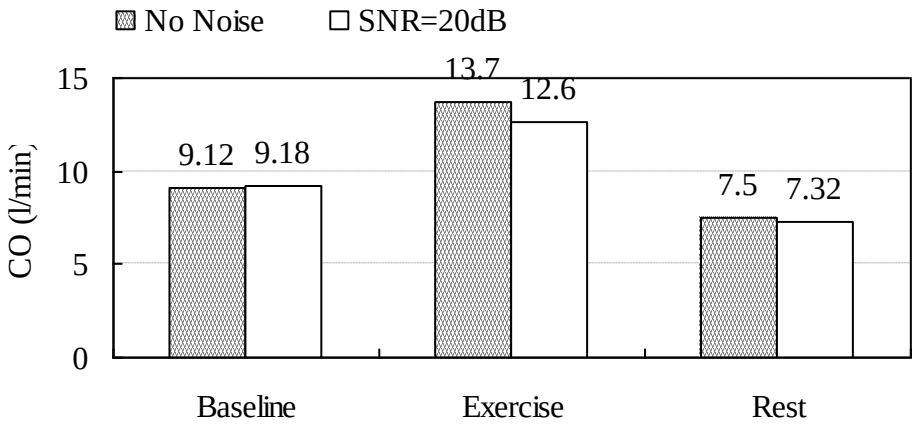

(a) Cardiac Output

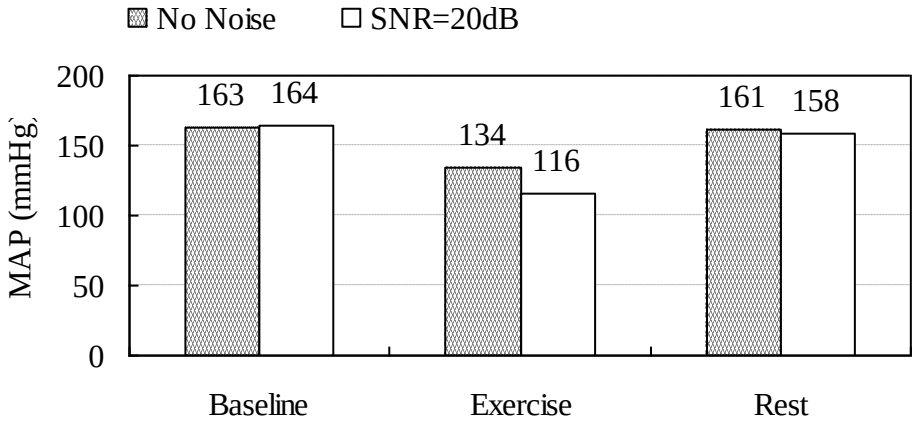

(b) Mean Arterial Pressure

FIGURE 4.16 Hemodynamic Variables Comparison without Noise and with SNR = 20 dB

4.2.3.3 Simulation Results With SNR = 10 dB

Once SNR decreases to only 10 dB, measurement noise may affect the simulation results more clearly than those with higher SNR, especially in the constant SVR case, the pump speed signals in Figure 4.17 (a) vary at nearly all the simulation time. Clearly there is still no suction phenomenon according to the net pump flow in Figures 4.17 (b) and 4.18 (b), however, at this time it is hard to make very clear distinction between the actual pump flow signals with noise in Figures 4.17 (c) and 4.18 (c) and the net pump flow since SNR = 10 dB means a high noise level. Moreover, sometimes the values of the actual pump flow with noise are negative, but these are not "backflow", the reason why the negative spikes occur is that noise with high level (corresponding to SNR = 10 dB) is added to the net pump flow.

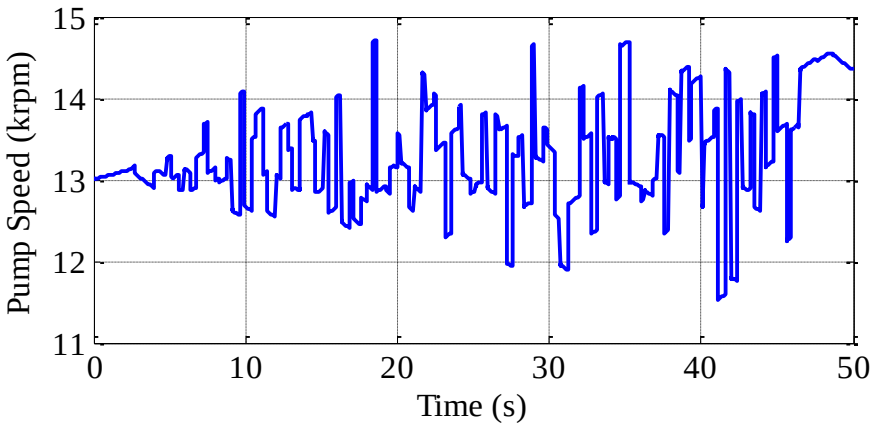

(a) Pump Speed

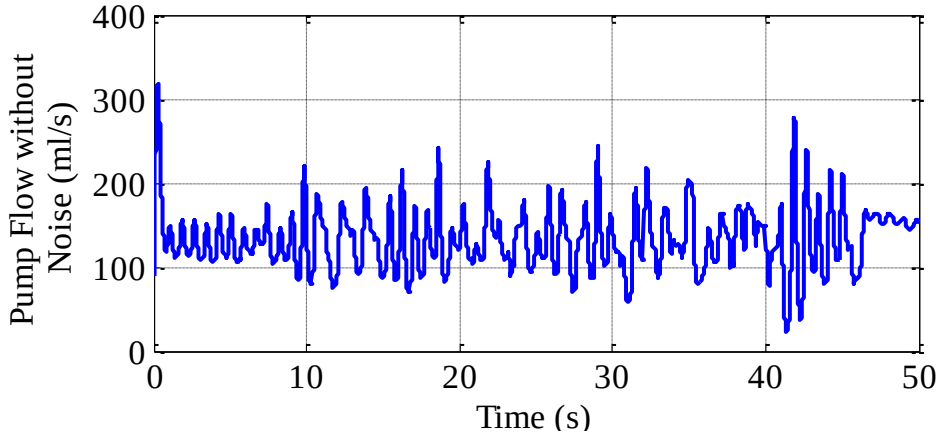

(b) Pump Flow without Noise

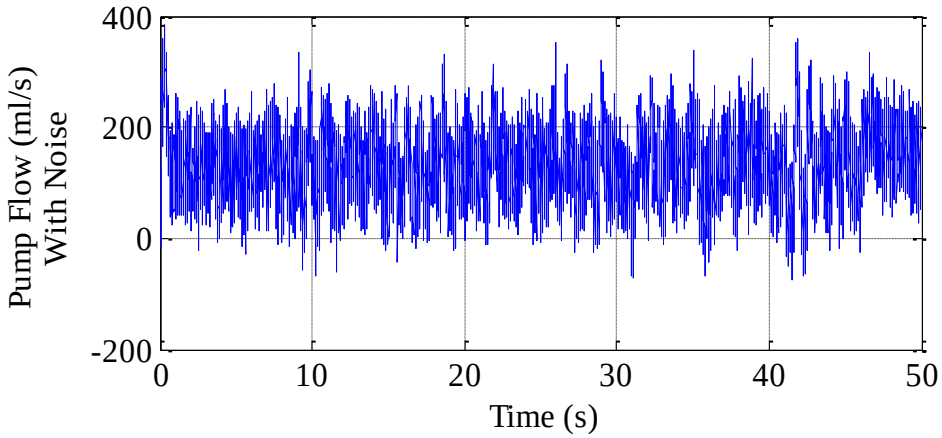

(c) Pump Flow with Noise

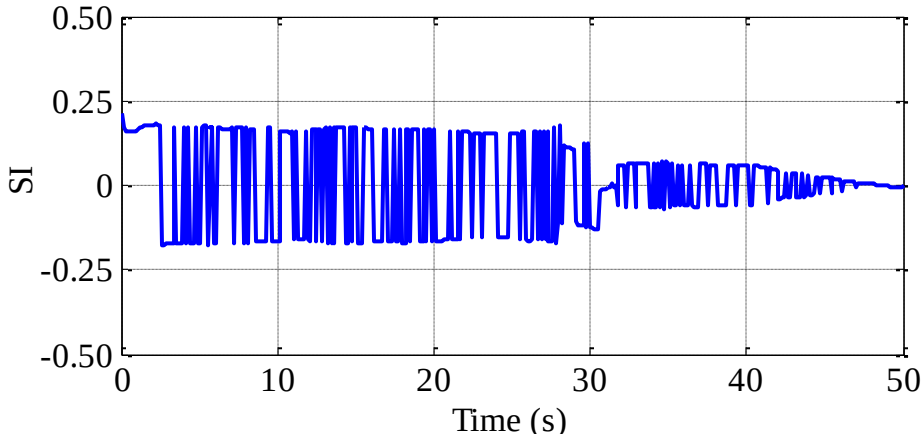

(d) Calculated SI

FIGURE 4.17 Simulation Results of Constant SVR with SNR = 10 dB

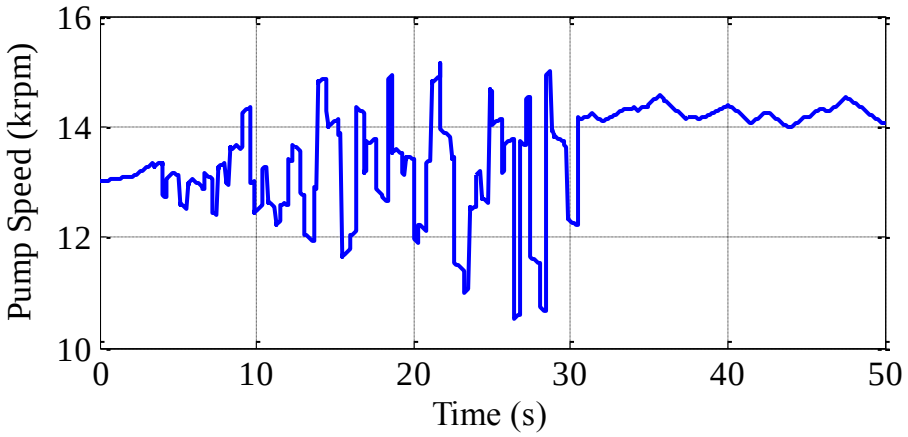

(a) Pump Speed

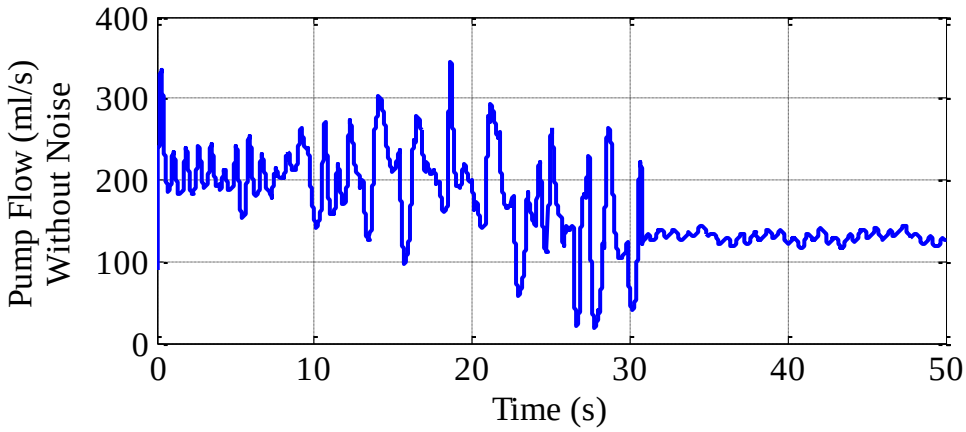

(b) Pump Flow without Noise

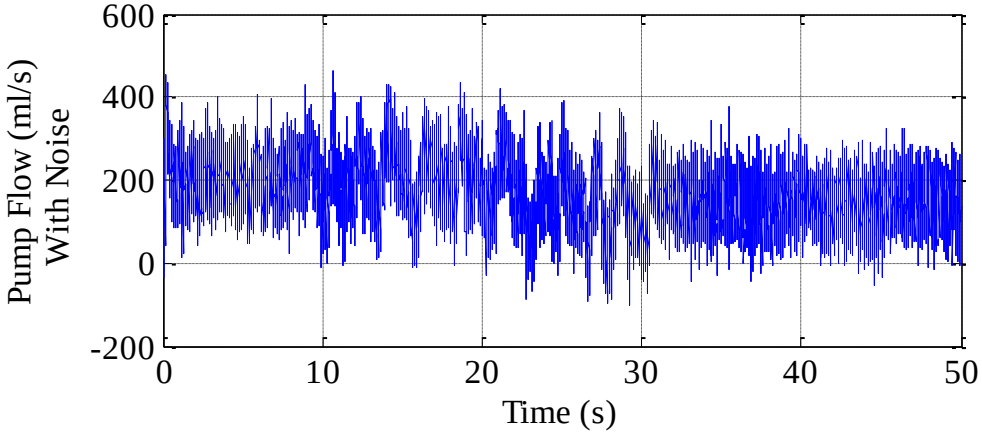

(c) Pump Flow with Noise

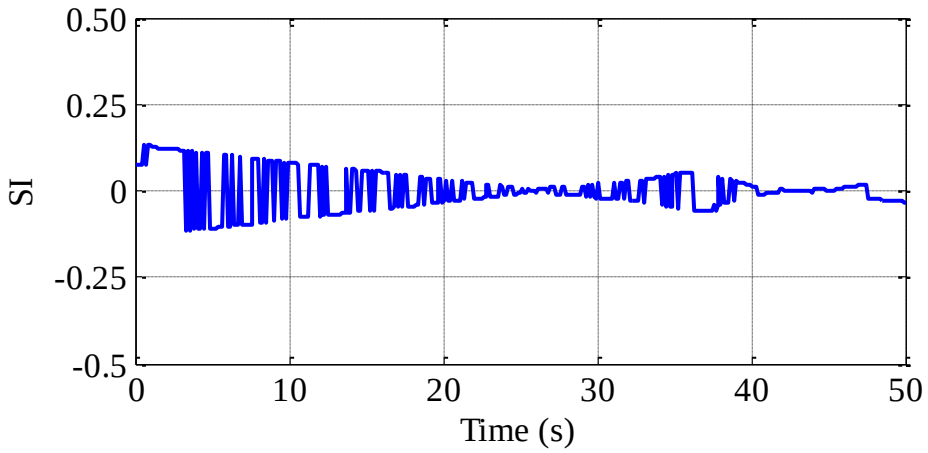

(d) Calculated SI

FIGURE 4.18 Simulation Results of Changing SVR with SNR = 10 dB

When SNR reduces to 10 dB, in the baseline level, CO and MAP decrease to 8.16 l/min and 147 mmHg respectively compared with all the previous results. Under the exercise condition, CO and MAP are the same as these with SNR = 20 dB (i.e., CO is 12.6 l/min and MAP is 116 mmHg). Under the rest condition, CO is 8.22 l/min and MAP is 176 mmHg, a little larger than any other previous result with the noiseless condition, SNR = 30 dB, and SNR = 20 dB. Note that the lower SNR, the greater influence on the measured results. All the results are shown in Figure 4.19 (a) for CO and 4.19 (b) for MAP in contrast to CO and MAP without noise.

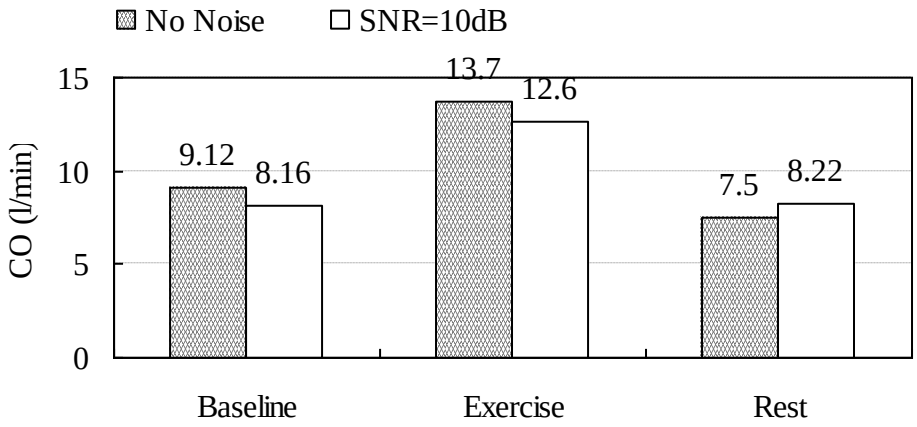

(a) Cardiac Output

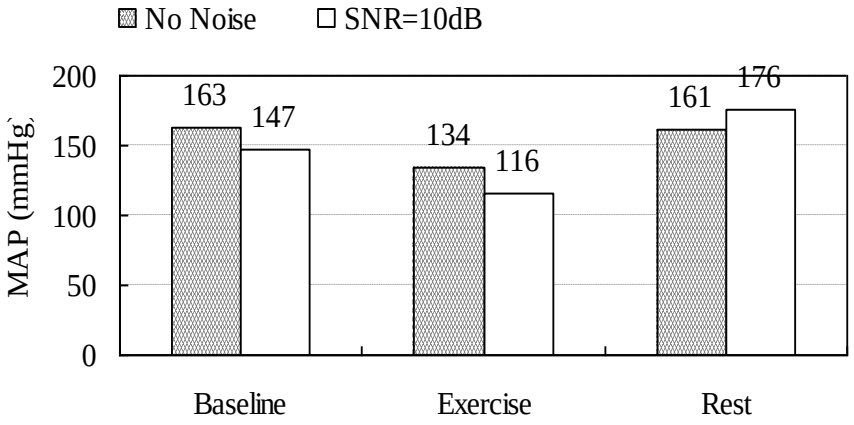

(b) Mean Arterial Pressure

FIGURE 4.19 Hemodynamic Variables Comparison without Noise and with SNR = 10 dB

4.2.3.4 Simulation Results With SNR = 5 dB

Figures 4.20 and 4.21 show the simulation results with uniformly distributed random noise at SNR = 5 dB for constant and changing SVR values, respectively. During the entire simulation period of time, in both Figures 4.20 (a) and 4.21 (a), the changes in the pump speed occur most

frequently compared with all the pump speed signals discussed previously. Furthermore, both suction and backflow occur under the varying SVR condition shown in Figure 4.21 (a) and (b) since the 5 dB-SNR corresponds to an extreme high noise level. In addition, the pump flow signals with noise are completely different from those without noise. In this case, the controller is negatively affected by this extreme low SNR and it couldn't perform as expected.

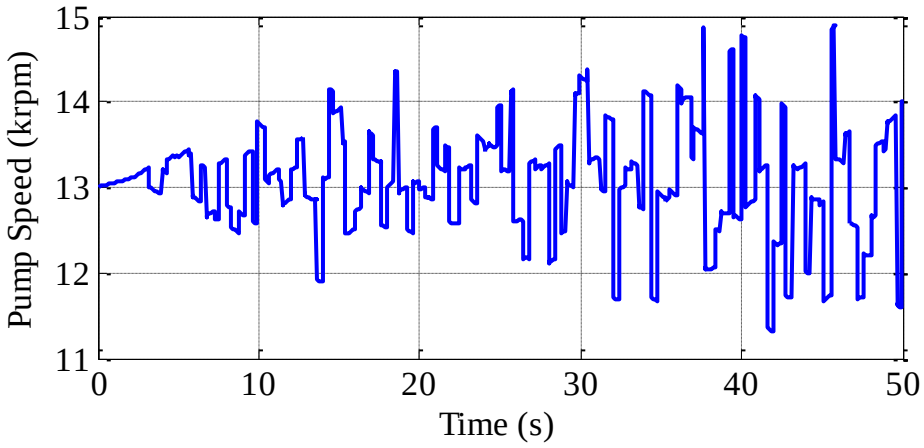

(a) Pump Speed

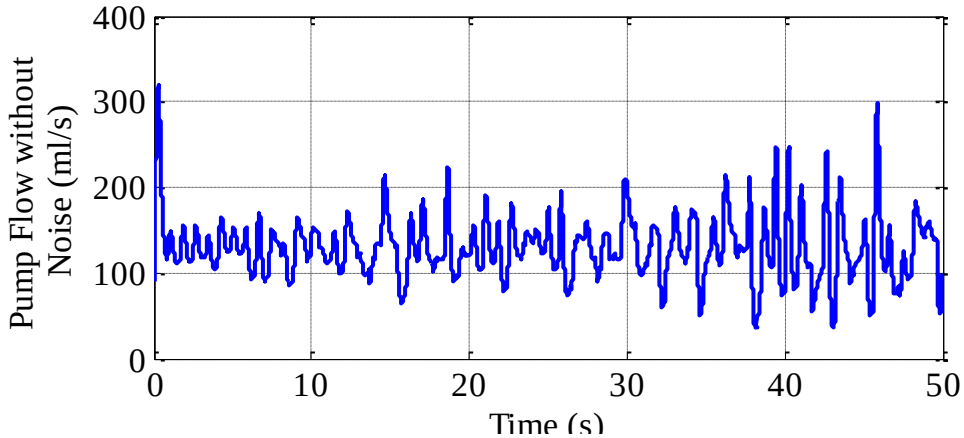

(b) Pump Flow without Noise

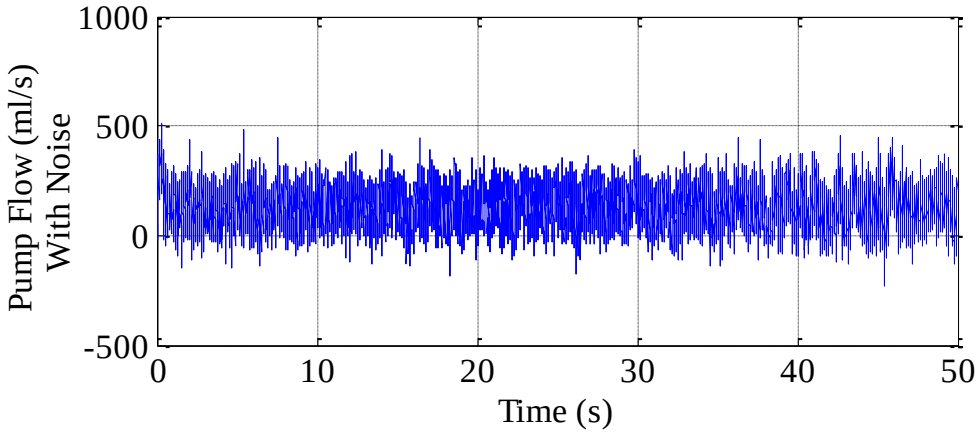

(c) Pump Flow with Noise

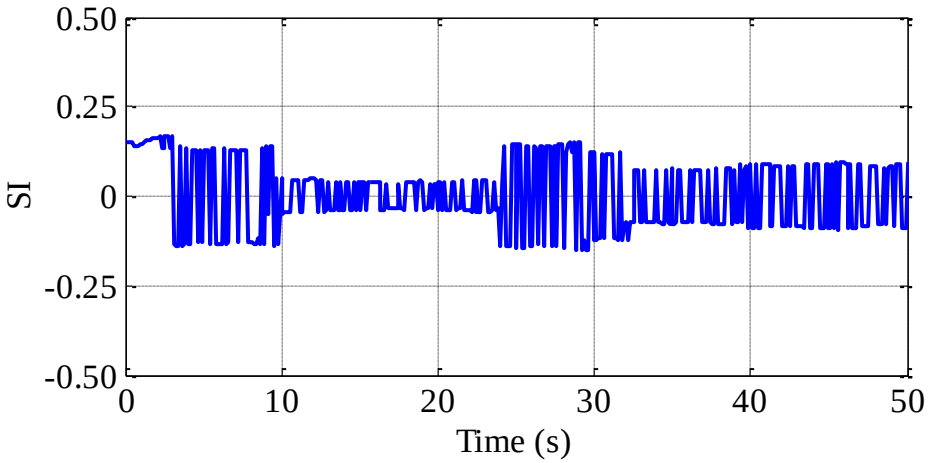

(d) Calculated SI

FIGURE 4.20 Simulation Results of Constant SVR with SNR = 5 dB

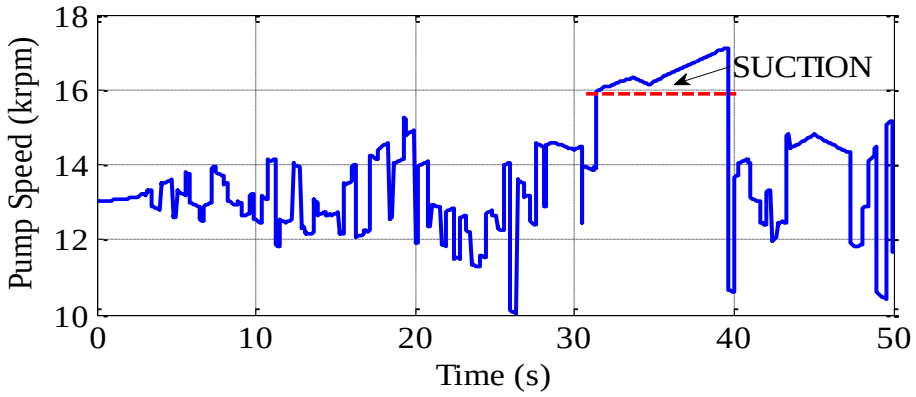

(a) Pump Speed

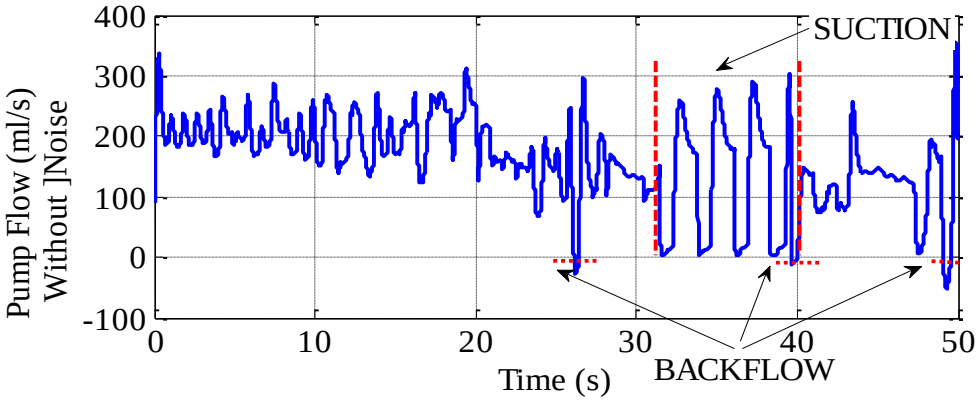

(b) Pump Flow without Noise

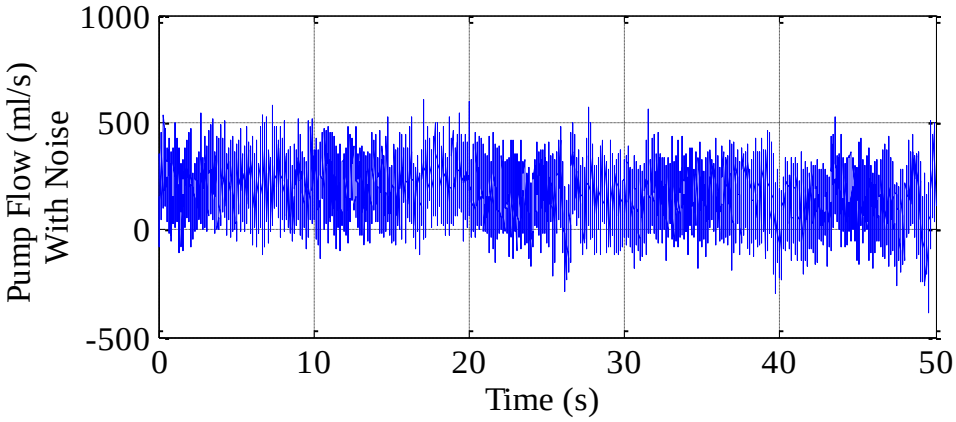

(c) Pump Flow with Noise

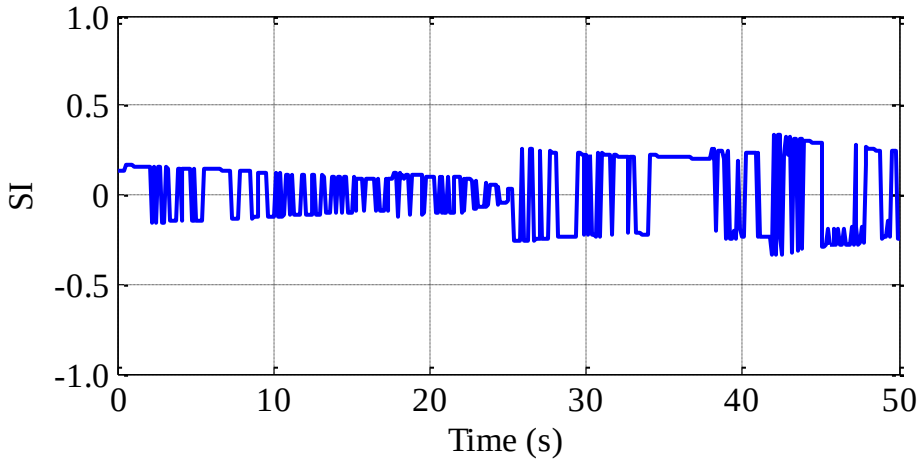

(d) Calculated SI

FIGURE 4.21 Simulation Results of Changing SVR with SNR = 5 dB

Figure 4.22 (a) and (b) illustrates CO and MAP without noise and those with SNR = 5 dB, notice that with SNR = 5 dB, both suction and backflow occur with changing SVR values; hence the two phenomena are taken into account for measurements. When R_S equals to 1.0mmHg.s/ml, CO and MAP still decrease to 7.9 l/min and 143 mmHg, respectively. These two parameters have no change in the exercise level compared these with SNR equals to 20 dB and 10 dB as still to be 12.6 l/min and 116 mmHg, respectively. When the patient is resting, CO is 7.7 l/min and MAP is 166 mmHg.

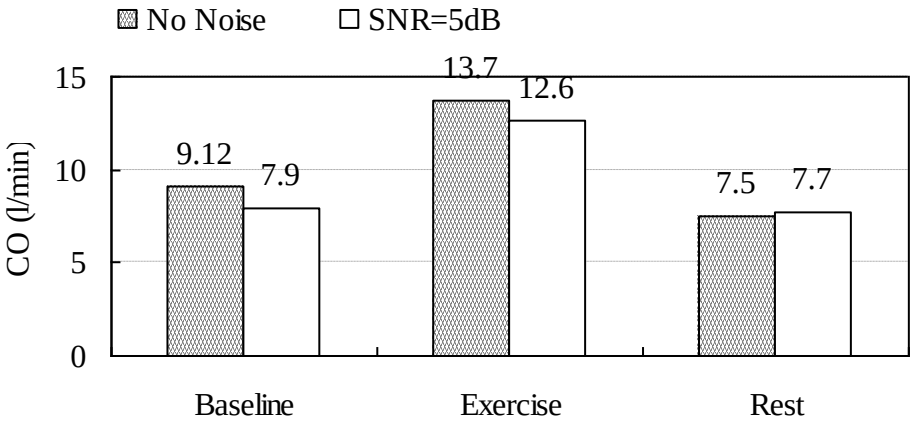

(a) Cardiac Output

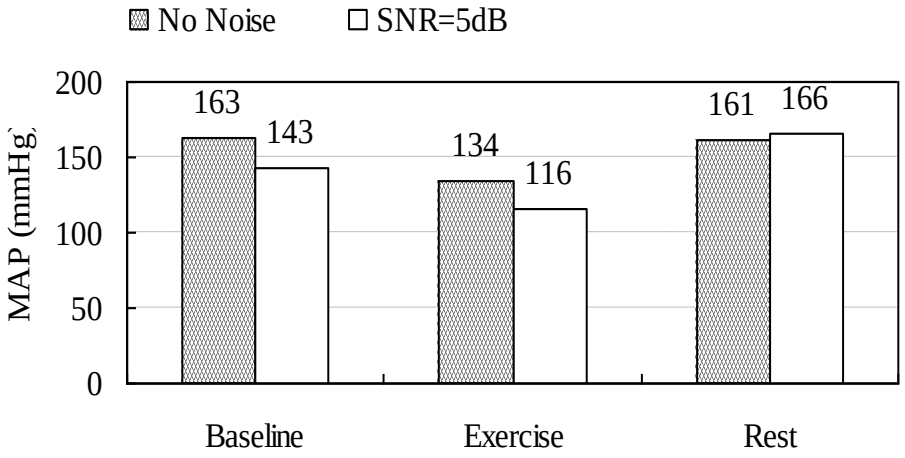

(b) Mean Arterial Pressure

FIGURE 4.22 Hemodynamic Variables Comparison without Noise and with SNR = 5 dB

TABLE 4.1 Response to Change in SNR

SNR (dB)	30	20	10	5	Tendency
Baseline CO (l/min)	9.7	9.18	8.16	7.9	Down
Baseline MAP (mmHg)	173	164	147	143	Down
Exercise CO (l/min)	14	12.6	12.6	12.6	Down then same
Exercise MAP (mmHg)	128	116	116	116	Down then same
Rest CO (l/min)	7.9	7.32	8.22	7.7	Varying
Rest MAP (mmHg)	170	158	176	166	Varying
Suction	No	No	No	Yes	-
Backflow	No	No	No	Yes	-

Table 4.1 lists the response to the changes in SNR. In conclusion, the controller can provide sufficient cardiac output and perfusion pressure under patients' changing physiological conditions no matter whether there is noise compared with these generated by a healthy heart, and the controller can satisfactorily deal with the SNR levels higher than 10 dB. Backflow and suction occur at SNR = 5 dB, however, in real-time the SNR levels measured in the blood flow sensors are always higher than 10 dB hence all the results shown above are acceptable.

CHAPTER 5:CONCLUSION AND FUTURE WORK

5.1 Conclusion

The development of an appropriate control system for rotary LVAD, which is capable of automatically adjusting the pump speed to support the patient with congestive heart failure, is an important challenge in some related research areas such as bioengineering, control system, etc. To meet this challenge, in this thesis, a new development of feedback controller for rotary LVAD was presented.

5.1.1 Cardiovascular-LVAD Model

To represent how to mimic the heart, a fifth-order uni-ventricular cardiovascular model was reviewed in this thesis. After that, a rotary blood pump, connected as a bridge between the left ventricle and the aorta, was discussed as the rotary LVAD to assist the sick heart. The combined cardiovascular-LVAD model in this thesis consists of six state variables: five (x_1 through x_5) in the fifth-order cardiovascular circuit model and the blood flow through the rotary pump (x_6). In the simulations, since the aortic pressure is always larger than the left ventricular pressure, the LVAD can totally support the sick heart, which implies that the cardiac output can be completely provided by the LVAD.

5.1.2 Suction Detection Problems

Suction is a very dangerous phenomenon in cardiovascular physiology, it must be avoided during the operation of LVAD. The suction detection system in this thesis relies on the pump flow signal (x_6), which is the only continuously measurable state variable with current implantable sensor technology in real-time. A special criterion, named "Mean-Min-Max", related to the mean, minimum, and maximum values of the pump flow signals within each cardiac cycle was reviewed and further studied. Once suction occurs, the mean value of the pump flow will be clearly close to the maximum value of the pump flow. Based on this characteristic, a corresponding Suction Index (SI) was tested to detect suction. Simulation studies for both in-vivo and model tests have proven the effectiveness of this suction index.

5.1.3 Feedback Controller

Depending on the aforementioned information, a feedback controller was proposed to continuously update the pump speed to avoid suction. In order to determine how to update the pump speed, a threshold associated with the suction index was presented as a rule to control the pump speed. If the value of the suction index is no more than that of the threshold, the controller can increase the pump speed, or the pump speed should be decreased. The choice of the threshold is crucial, with much larger value of it compared with that of the suction index, the pump speed needs to increase until the suction index catches up with the threshold. Therefore,

suction may occur if the pump speed increases to a certain value that is in the suction speed region. Likewise, for the smaller threshold, the blood may regurgitate from the aorta to the left ventricle, known as “backflow” due to the decreasing pump speed.

5.1.4 Related Simulation Studies

To check the performance of this controller, simulations were implemented under both constant and varying patient activity levels (baseline, exercise, and rest conditions) for a sick heart. Suction does not occur during the simulations. Furthermore, since another objective of the controller is to guarantee that it can provide adequate Cardiac Output (CO) and Mean Arterial Pressure (MAP), hence the corresponding analysis for CO and MAP is presented. Simulation results show that the controller can provide larger CO and MAP compared with the two hemodynamic parameters supported by a healthy heart.

In practice, the blood flow sensors clinically used always contain noise with different SNR values; hence testing the robustness of the controller to measurement noise is necessary. Uniformly distributed random noise was adopted in the simulations. Simulation studies show that the controller is robust to noise added to the pump flow signal until SNR is less than 10 dB, a very low SNR level than generally obtained in the blood flow sensors clinically implanted. When the SNR level is less than 10dB (e.g. SNR = 5 dB), measurement noise can disrupt the

suction index, causing the pump speed to be updated incorrectly, as a result, both backflow and suction can occur.

5.1.5 Limitations

So far, the work only has been done with the model simulations. In the simulations, the heart rate is assumed to be constant (75 bpm) and three typical values of SVR are chosen to express the baseline, exercise, and rest conditions as the patient different activity levels. However, in real-time, measuring these variables may be very complicated, especially in the case of the heart rate, it may be always changing under the patient's varying physiological conditions. Moreover, for patients with heart failure, it is most likely that there are various kinds of premature beats or miss beats (e.g. atrial, ventricular, etc), which make measurements for the heart rate more difficult than that obtained based on the model simulation.

In addition, besides the case of heart rate, in real life different patients may need different thresholds and adjustment parameter gains to be set due to individual physiological feature. In this thesis, the controller can work well but the pump speed cannot be definitely stable although the changing range in the pump speed is very small without noise. However, when adding noise to the pump flow signal, the pump speed signals fluctuate more frequently than these without noise.

5.2 Future Work

Based on the limitations above, in the future:

(1) The changing heart rate instead of the constant can be applied to the cardiovascular-LVAD model in order that the model can mimic the patient's physiological condition as practically as possible. For instance, in the baseline level, HR is 75 bpm but under the exercise condition, HR may change to be 90 bpm or more.

(2) To avoid the adverse phenomenon of suction, some new approaches could be used to detect suction such as Neural Network (NN) or Support Vector Machine (SVM) that is a powerful method with more features extracted from the pump flow or other available signals.

(3) To classify the states of the pump flow or other available signals more clearly and correctly, the signal status can be divided into three categories: no suction, close to suction, severe suction, instead of only no suction and suction.

(4) Based on the suction detection, the related control algorithm can be developed and incorporated as part of the more sophisticated, precise, and stable controller for rotary blood pumps.

LIST OF REFERENCES

[1] Gu, M. and Qin, Y., "Development of left ventricular assist devices," International Journal of Cardiovascular Disease, 36(2): 69-71, 2009.

[2] http://www.americanheart.org/presenter.jhtml?identifier=4599

[3] Slaughter, M. S., Rogers, J.G., et al, "Advanced heart failure treated with continuous-flow left ventricular assist device," The new England journal of medicine, Nov. 17, 2009.

[4] Vollkron, M., Schima, H., Huber, L., Benkowski, R., Morello, G., et al, "Development of a suction detection system for axial blood pumps," Artificial Organs, 28(8): 709-716, 2004.

[5] Vollkron, M., Schima, H., Huber, L., Benkowski, R., Morello, G., et al, "Advanced suction detection for an axial flow pump," Artificial Organs, 30(9): 665-670, 2006.

[6] Voigt, O., Benkowski, R.J. and Morello, G.F., "Suction detection for the micromed debakey left ventricular assist device," ASAIO Journal, 51(4): 321-328, 2005.

[7] Ferreira, A., Chen, S., Simaan, M.A., Boston, J.R. and Antaki, J.F., "A discriminant-analysis-based suction detection system for rotary blood pump," Proceedings of the IEEE EMBC, New York, USA, 5382-5385, 2006.

[8] Mason, D.G., Hilton, A.K. and Salamonsen, R.F., "Reliable suction detection for patients with rotary blood pumps," ASAIO Journal, 54(4): 359-366, 2008.

[9] Wu, Y., Allaire, P., Tao, G., Wood, H., Olsen, D. and Tribble, C., "An advanced physiological controller design for a left ventricular assist device to prevent left ventricular collapse," Artificial Organs, 27(10): 926-930, 2003.

[10] Vollkon, M., Schima, H., Huber, L., Benkowski, R., Morello, G., et al, "Development of a reliable automatic speed control system for rotary blood pumps," The Journal of Heart and Lung Transplantation, 24(11): 1878-1885, 2005.

[11] Chen, S., "Baroreflex-based Physiological Control of a Left Ventricular Assist Device," University of Pittsburgh, 2006.

[12] Chen, S., Ferreira, A., Simaan, M.A., Boston, J.R. and Antaki, J.F., "Feedback control of an LVAD supporting a failing cardiovascular system regulated by a baroreflex," Proceedings of the 45th IEEE CDC, San Diego, CA, USA, Dec. 13-15: 655-660, 2006.

[13] Ferreira, A., "A rule-based controller based on suction detection for rotary blood pumps," PhD. Thesis, University of Pittsburgh, Pittsburgh, PA, 2007.

[14] Ferreira, A., Boston, J.R., and Antaki, J.F., "A control system for rotary blood pumps based on suction detection," IEEE Transactions on Biomedical Engineering, 56(3): 656-665, 2009.

[15] Simaan, M.A., Ferreira, A., Chen, S., Antaki, J.F. and Galati, D.G., "A Dynamical State Space Representation and Performance Analysis of a Feedback-Controlled Rotary Left

Ventricular Assist Device," IEEE Transactions on Control Systems Technology, 11(7): 15-28, 2009.

[16] http://www.zgxl.net/sljk/imgbody/xinzang.htm

[17] http://en.wikipedia.org/wiki/File:Heart_systole.svg

[18] http://en.wikipedia.org/wiki/File:Heart_diastole.png

[19] http://www.hudong.com/wiki/%E5%BF%83%E5%8A%A8%E5%91%A8%E6%9C%9F

[20] Suga, H., Sagawa, K., "Instantaneous pressure-volume relationships and their ratio in the excised, supported canine left ventricle," Circulation Research, 35(1): 117-126, 1974.

[21] Stergiopulos, N., Meister, J. and Westerhof, N., "Determinants of stroke volume and systolic and diastolic aortic pressure," American Journal of Physiology, 270(6): 2050-2059, 1996.

[22] Simaan, M.A., "Modeling and control of rotary heart assist device," Handbook of Automation, Ed S. Norf, Springer Verlag, 1409-1422, 2009.

[23] Schima, H., Trubel, W., Moritz, A., et al, "Noninvasive monitoring of rotary blood pumps: necessity, possibilities, and limitations," Artificial Organs, 16(2): 195-202, 1992.

[24] Yuhki, A., Hatoh, E., Nogawa, M., Miura, M., Shimazaki, Y. and Takatani, S., "Detection of suction and regurgitation of the imiplantable centrifugal pump based on the motor current waveform analysis and its application to optimization of pump flow," Artificial Organs, 23(6): 532-537, 1999.

[25] Morello, G.F., "Blood pump system and method of operation," US Patent: 0215050, 2004.

[26] Karantonis, D.M., Lovell, N.H., Ayre, P.J., Mason, D.G. and Cloherty, S.L., "Identification and classification of physiologically significant pumping states in an implantable rotary blood pump," Artificial Organs, 30(9): 671-679, 2006.

[27] K., M., "Central venous pressure and pulmonary capillary wedge pressure monitoring," Indian Journal of anaesthesia, 46(4): 298-303, 2002.

[28] Klabunde, R.E., "Cardiovascular physiology concepts," Lippincott Williams & Wilkins, 2005

[29] http://www.doctorsky.cn/surgery/20081029/51524.html